Atmos. Chem. Phys. Discuss., 15, 11925–11983, 2015
www.atmos-chem-phys-discuss.net/15/11925/2015/
doi:10.5194/acpd-15-11925-2015

Atmospheric Chemistry and Physics Discussions

Observations of atmospheric mercury in China: a critical review

X. W. Fu[1], H. Zhang[1,2], X. Wang[1,2], B. Yu[1,2], C.-J. Lin[1,3,4], and X. B. Feng[1]

[1]State Key Laboratory of Environmental Geochemistry, Institute of Geochemistry, Chinese Academy of Sciences, Guiyang 550002, China
[2]Graduate University of the Chinese Academy of Sciences, Beijing 100049, China
[3]Department of Civil Engineering, Lamar University, Beaumont, TX 77710, USA
[4]College of Energy and Environment, South China University of Technology, Guangzhou 510006, China

Received: 28 January 2015 – Accepted: 7 April 2015 – Published: 22 April 2015

Correspondence to: X. B. Feng (fengxinbin@vip.skleg.cn)

Published by Copernicus Publications on behalf of the European Geosciences Union.

Abstract

China is presently the largest contributor of global anthropogenic Hg emission to the atmosphere. Over the past two decades, extensive studies have been conducted to characterize the concentration and speciation of atmospheric Hg in China. These studies provide important insight into the spatial and temporal distributions of atmospheric Hg species in China through ground-based measurements at a wide range of altitude over diverse geographical locations, and cruise and flight campaigns. In this critical review, we synthesize the available data to date to delineate the spatial and temporal patterns of atmospheric Hg, the long-range transport pattern of atmospheric Hg, and the impacts of Hg emissions on atmospheric Hg distribution and deposition in China. Atmospheric Hg species in China are substantially elevated compared to the background values in the Northern Hemisphere. The highly elevated Hg levels in Chinese urban areas were derived from local and regional anthropogenic and natural emissions, while long-range transport plays an important role in the atmospheric Hg concentration in remote areas. Preliminary studies suggested that atmosphere GEM levels are increasing at an urban and remote sites over the last decade, which were likely caused by the increasing anthropogenic emissions. The anthropogenic emission quantity in China estimated through the observed concentration ratios of GEM to CO (observed from 2001 to 2013) is approximately 983 t in 2009, ~ 3 folds of the published anthropogenic GEM emission inventories using activity data. Wet deposition fluxes of Hg in remote regions are low but the fluxes in Chinese urban areas are much higher than that in urban areas of North America and Europe. Dry deposition fluxes of Hg measured as litterfall input in forest areas of China were 2.5–9.0 times higher than the wet deposition fluxes and 1.8–13.6 times higher than the dry deposition fluxes of Hg in North America and Europe, suggesting that dry deposition to forest may be an important sink of atmospheric Hg in China.

ACPD
15, 11925–11983, 2015

1 Introduction

Mercury (Hg) is a highly toxic heavy metal pollutant that exists mainly in the gaseous phase of the atmosphere. There are three major operationally defined Hg forms, namely gaseous elemental mercury (GEM), particulate bounded mercury (PBM), and gaseous oxidized mercury. The sum of GEM and GOM is known as total gaseous mercury (TGM). Because of its mild reactivity, high volatility, and low dry deposition velocity and water solubility, GEM is the most abundant form of Hg species in the atmosphere. GEM is believed to have a long residence time (0.5–2 years) and can spread globally before being transformed to other atmospheric Hg species and deposited to earth's surfaces (Schroeder and Munthe, 1998). Recent studies have observed fast transformations of GEM to GOM and PBM in the polar regions, upper free troposphere, lower stratosphere, and marine free troposphere, indicating a much shorter atmospheric residence time of GEM in these environments (Schroeder et al., 1998; Hedgecock and Pirrone, 2003; Lyman and Jaffe, 2012; Timonen et al., 2013; Murphy et al., 1998). On the other hand, GOM and PBM have much higher dry deposition velocity and water solubility and can be readily scavenged from the atmosphere. Hg is one of the most widely distributed pollutants in the environment because of these unique characteristics.

Both anthropogenic (e.g., coal combustion, non-ferrous metal production, cement production, mercury production, Caustic soda production) and natural sources (e.g. evasion from soils, water bodies, forest fire, volcanoes) emit GEM to the atmosphere, while anthropogenic sources also emit a large amount of GOM and PBM (Pirrone et al., 2010; Pacyna et al., 2010). Due to the direct emission and re-emission of anthropogenic sources, the budget of atmospheric Hg has been increased by a factor of 3 since the onset of industrial revolution (Mason and Sheu, 2002). During the past decades, many control measures have been taken to reduce anthropogenic Hg emissions in Europe and North America, which led to a significant decrease in atmospheric TGM concentrations in Europe and North America (Slemr and Scheel, 1998; Slemr et al., 2003; Cole et al., 2013). However, due to the increasing consumption of energy

ACPD
15, 11925–11983, 2015

and lower implementation of pollution control devices, anthropogenic emissions in Asia appeared to increase during the past decades and play a more important role in the global Hg cycle (Wu et al., 2006; Liang et al., 2013). China is regarded as the world largest anthropogenic source region of atmospheric mercury. Recent estimates suggest that anthropogenic emissions of Hg to the atmosphere are in the range of from 500 to 1000 $t\,yr^{-1}$ (Streets et al., 2005; Wu et al., 2006; Liang et al., 2013), approximately 1/3 of the total global anthropogenic emissions. Information on natural emissions (including direct natural and legacy emissions) of Hg in China is limited. GEM emission fluxes from various landscapes in China were summarized by Fu et al. (2015) and significantly higher than that observed from Europe and North America.

There is a need to assess the source, deposition, distribution, transport, and atmospheric processes of atmospheric Hg in China, which is important for better understanding of the global biogeochemical cycle of Hg in the environment. During the last two decades, studies on atmospheric Hg in China have focused on the distributions and transport of atmospheric Hg at ground-based sites, and in coastal and open sea areas, upper troposphere, and lower stratosphere. Additionally, measurements of atmospheric deposition in various areas of China were also conducted. These efforts elucidated the three dimensional distributions of atmospheric Hg in China, constrained the inventory of Chinese Hg emissions, assessed the transport of atmospheric Hg in China, and evaluated the role of Chinese emissions in regional- and global-scale Hg cycle. In this paper, we provide an integrated synthesis on the state of understanding in atmospheric Hg in China.

ACPD
15, 11925–11983, 2015

2 Observational approaches

2.1 Atmospheric total gaseous mercury (TGM) and gaseous elemental mercury (GEM)

There are a number of methods utilized for measurements of atmospheric Hg in China. For atmospheric TGM and GEM, the most widely utilized method is the commercial Model 2537 A/B automated ambient mercury vapor analyzer (Tekran, Canada). This automated analyzer combines the pre-concentration of Hg vapor (GEM and a fraction of GOM) on dual gold cartridges, thermal desorption and detection of Cold Vapor Atomic Fluorescence Spectrometry (CVAFS), periodic auto calibrations using internal permeation source and manual calibration using external Hg vapor standard (e.g. Tekran Model 2505 calibration unit) in a single package that enables continuous measurements of atmospheric Hg vapor. This analyzer is believed to provide accurate measurement of atmospheric Hg vapor and has a detection limit of $\sim 0.1\,\mathrm{ng\,m^{-3}}$ as specified by Tekran Instrument Corporation. There have been debates as to whether the Tekran Model 2537 measures TGM (the sum of GEM and GOM) or GEM. It has been suggested that, in certain conditions such as marine boundary layer with large salt aerosols, humid ambient air, installation of soda lime trap and using of unheated Teflon sampling tube, GOM in ambient air is not likely to bypass the sampling line and filter and therefore the measurement is GEM (Fu et al., 2010b; Moore et al., 2013). For other instances, the measured atmospheric Hg vapor likely represents TGM. It should be pointed out that GEM concentration in remote areas is approximately two orders of magnitude higher than the GOM level, and therefore the measurement of TGM or GEM does not yield significant errors. In this review, we refer the atmospheric TGM and GEM observations in China to GEM for text clarity and consistency.

RA-915 +Hg analyzer (Lumex, Russia) has also been used for monitoring of GEM in several Chinese studies (Yang et al., 2009; Ci et al., 2011a, b). It is based on differential Zeeman Atomic Absorption Spectrometry with High-Frequency Modulation of light polarization (ZAAS–HFM) and a multi-path analytical cell. This analyzer can measure

ACPD
15, 11925–11983, 2015

GEM at a very short interval of 1 s and has a detection limit from 0.3 to 1.0 ng m^{-3} (Ci et al., 2011a). Previous studies revealed that the RA-915 +Hg analyzer has a good agreement with the traditional gold trap/CVAFS method and Tekran 2537 automated analyzer for GEM measurements in urban environment for GEM concentrations ranging from 1 to 100 ng m^{-3} (Kim et al., 2006; Fu et al., 2011b). However, further field intercomparisons are needed for validating RA-915 +Hg analyzer's performance at remote and/or high-altitude sites. Other studies in China used a manual method which collects GEM on gold-coated beads or sand traps, followed by thermal desorption and detection of CVAFS (Fang et al., 2004; Xiang and Liu, 2008). This is a standard manual method and compares well with automated GEM analyzers (Ebinghaus et al., 1999).

2.2 Atmospheric gaseous oxidized mercury (GOM) and particulate bounded mercury (PBM)

There are currently no standard methods for measurements of GOM and PBM in the atmosphere. This is mainly due to a combination of reasons including unknown chemical composition of GOM and PBM and a lack of reliable sampling and calibration techniques, and therefore the measurements of these two atmospheric Hg species (especially GOM) by previous studies are believed to be more or less qualitative.

For measurements of GOM and PBM in China, several studies utilized the Tekran 2537/1130/1135 automated speciation analyzer system (Tekran, Canada) (Fu et al., 2011a; Zhang et al., 2013). This system has been widely used and described in detail by many previous studies (Landis et al., 2002; Lindberg et al., 2002; Lan et al., 2012). Briefly, this system includes a KCl-coated quartz annular denuder and a quartz fiber filter, which allows the collection of GOM and PBM in sequence. Once collected, PBM and GOM are thermally desorbed from each unit and determined as GEM using the Tekran 2537 analyzer. Coarse particles with an aerodynamic size of > 2.5 µm is firstly removed by a glass inertial impactor prior to entering the system. Therefore, the PBM measured by this system represents fine (< 2.5 µm) particulate bounded mercury. The

ACPD
15, 11925–11983, 2015

detection limits of GOM and PBM using the system have been reported to be 0.5–6 pg m^{-3}, which is partially depending on the sampling duration (Landis et al., 2002; Poissant et al., 2005). It is worth noting that many recent studies suggested there are uncertainties about GOM measurements using Tekran system. This is mainly due to the lack of calibration standards of GOM and PBM, incomplete collection and loss of atmospheric GOM and PBM during sampling (Jaffe et al., 2014; Gustin et al., 2015). Recent filed and laboratory intercomparison studies suggested that the GOM measured by Tekran system may be biased low by a factor of 1.6–10.6 times as compared to newly developed methods such as Detector for Oxidized Hg Species (DOHGS), nylon membranes and cation exchange membranes, and the biased factor can be influenced by the form of GOM, Ozone and relative humidity (Lyman et al., 2010; Huang et al., 2013; Gustin et al., 2013; Ambrose et al., 2013; McClure et al., 2014).

A manual method similar to the Tekran 2537/1130/1135 system has also been applied to measure GOM and PBM in China (Fu et al., 2012a; Zhang et al., 2015a). This method collects GOM and PBM (fine particulate bounded mercury) onto a KCl-coated quartz annular denuder and a quartz fiber filter in sequence. After sampling, annual denuder and quartz fiber filter (transported manually into a quartz tube) are flushed with zero gas, followed by thermal desorption at required temperature which converts GOM and PBM into GEM for CVAFS detection. The detection limits of GOM and PBM based on 3 times the SDs of blanks are 1.2 and 4.2 pg m^{-3}, respectively (Fu et al., 2012a).

Total particulate bounded mercury (TPM) has also been measured in China. In these studies, airborne particles were collected onto glass and/or quartz fiber filter without any upstream cut-off devices. For determination of TPM concentrations, Fu et al. (2008c) and Xu et al. (2013) used a thermal desorption coupled with detection by Tekran 2537 analyzer and Lumex RA-915 +Hg analyzer, while other studies used acid digestion and CVAFS detection (Fang et al., 2004; Wang et al., 2006b; Xiu et al., 2009). The thermal desorption method yields relatively lower (30–56 %) values for particulate

ACPD
15, 11925–11983, 2015

bounded mercury when compared with acid digestion (Lynam and Keeler, 2002), likely due to the matrix interference of gold traps and/or blank of chemical reagents.

2.3 Atmospheric wet deposition

Wet deposition flux of atmospheric Hg can be estimated via periodical or event-based measurements of precipitation Hg concentrations and rainfall depth. Previous studies in China used both bulk collector (Fu et al., 2008c; Guo et al., 2008; Wan et al., 2009a; Fu et al., 2010a) and wet-only collector (Fu et al., 2010b; Liu et al., 2011; Wang et al., 2012; Zhu et al., 2014; Zhou et al., 2013). Due to the dry deposition of atmospheric TPM during the sampling period, the bulk collector tends to overestimate the wet deposition flux. The artifact of using bulk collector may be lower at remote sites with low atmospheric TPM concentrations and a short sampling duration such as < 1 week (Landis and Keeler, 1997). Given that atmospheric TPM concentrations in China are generally elevated (Sect. 3.1), previous observations using bulk collectors likely overestimated the wet deposition fluxes. Analysis of total mercury (THg) and methyl mercury (MeHg) concentrations in precipitations in China followed the standard methods of EPA Method 1631B and Method 1630 (USEPA, 1998, 2002).

2.4 Atmospheric dry deposition

Dry deposition is an important pathway for the removal of atmospheric Hg and for the Hg input to ecosystems. Dry deposition velocities for atmospheric Hg are thought to vary significantly with the physical and chemical forms of atmospheric Hg, meteorological conditions, and surface characteristics (Gustin and Jaffe, 2010). Zhang et al. (2009) critically reviewed the dry deposition velocities of different atmospheric Hg forms. Using the measured concentrations of atmospheric Hg species in North America and its dry deposition velocities, Zhang et al. (2012) estimated the speciated and total mercury dry deposition fluxes in eastern and central North America. The result suggested that dry deposition flux of Hg is equal to or more than the wet deposition flux in North America.

ACPD
15, 11925–11983, 2015

Due to the direct and legacy emissions, the levels of GEM, GOM and PBM in China are highly elevated compared to those observed in North America. This indicates dry deposition of Hg may be more important in China. However, due to the lack of reliable database of speciated atmospheric Hg concentrations in ambient air and its dry deposition velocities, studies of dry deposition flux in China are limited. Several approaches have been attempted to predict the concentrations of speciated atmospheric Hg in ambient air and to empirically estimate dry deposition fluxes (Lin et al., 2010; Wang et al., 2014a). Due to the large discrepancy of speciated atmospheric Hg concentrations between modeling and observed observations, these may exist significant uncertainties in the estimates.

Dry deposition flux of Hg in forest ecosystem of China has also been investigated (Wang et al., 2009; Fu et al., 2010b, a). These studies was based on the measurements of deposition fluxes by throughfall and litterfall, which provide a good estimate of total dry deposition of atmospheric Hg in forest ecosystems (St Louis et al., 2001; Zhang et al., 2012). However, due to the incomplete understanding in the sources of Hg in litterfall, the exchange of Hg at air-leaf interface, the dry deposition to forest soil, these fluxes should be considered as approximate estimates.

3 Results and discussion

3.1 Atmospheric mercury at ground-based sites

3.1.1 Gaseous elemental mercury (GEM)

Extensive observations of atmospheric Hg speciation have been carried out at ground-based sites in China. Table 1 shows the statistical summary of speciated atmospheric Hg concentrations and associated site information. Averaged GEM concentrations at remote sites were in the ranges of 1.60–5.07 $\mathrm{ng\,m^{-3}}$ (mean = $2.86 \pm 0.95\ \mathrm{ng\,m^{-3}}$, n = 12), mostly elevated compared to those observed in North America, Europe, South

ACPD
15, 11925–11983, 2015

Africa and South America (Table 1). For example, average GEM concentrations at 11 of the 12 remote sites in China exceeded the background concentrations of GEM (1.5–1.7 ng m^{-3}) in the Northern Hemisphere (Lindberg et al., 2007).

Significant variation of GEM concentrations was also observed at the remote sites in China (Fig. 1). In general, GEM concentrations in northeast, northwest, and southwest China (e.g. Mt. Changbai, Mt. Waliguan, and Mt. Ailao, means = 1.60–2.09 ng m^{-3}) were relatively lower than those (2.94–5.07 ng m^{-3}) in northern, southern, and eastern China (e.g. Miyun, Mt. Damei, and Mt. Dinghu, Fig. 1). This pattern is similar to the spatial distribution of anthropogenic emissions in China (Wu et al., 2006; AMAP/UNEP, 2013). According to the Chinese anthropogenic Hg emission inventories, most of the anthropogenic mercury sources are located in northern, central, eastern, and southern China. The anthropogenic Hg emissions in northeast (Jilin and Heilongjiang province), western (Xinjiang, Xizang, and Qinghai province), and southwest China (mainly in Yunnan province) are relatively lower (Fig. 2). Mt. Gongga and Mt. Leigong in southwest China showed relatively higher GEM concentrations of 3.98 ± 1.62 ng m^{-3} and 2.80 ± 1.51 ng m^{-3}, respectively, approximately 2–3 times higher than the background level in the Northern Hemisphere. These two sites are located in Sichuan and Guizhou provinces, two of the largest anthropogenic sources regions in China (Wu et al., 2006). The highest average GEM concentration (5.07 ± 2.89 ng m^{-3}) at remotes of China was observed at Mt. Dinghu in the central Pearl River Delta (Chen et al., 2013). The Pearl River Delta is one of the most industrialized and urbanized regions in China. Total anthropogenic Hg emissions in the Pearl River Delta in 2008 were estimated to be 15.7 t (Zheng et al., 2011). Most of the emissions were located upwind of Mt. Dinghu, which may explain the elevated GEM concentrations observed at Mt. Dinghu. In addition, Hg emissions from natural surfaces cannot be ruled out. Due to the elevated geologic background of Hg in soil and reemissions of deposited mercury, GEM emissions from agricultural and bare soils in the Pearl River Delta were in the range of 18.2–135 ng m^{-2} h^{-1}, higher than that in southwest China and approximately one order

ACPD
15, 11925–11983, 2015

of magnitude higher than the observations in Europe and North America (Fu et al., 2012c).

Average GEM concentrations at the urban sites of China ranged from 2.50 to 28.6 ng m^{-3} (mean = 9.20 ± 7.56 ng m^{-3}, n = 13). Nine of the 13 urban sites showed average concentrations higher than the maximum values observed in North America and Europe (Table 1). Urban areas in China are densely populated and heavily industrialized. The high energy demand and the presence of other large point sources (e.g. iron and steel production, non-ferrous metals smelting, cement production) contribute to the large Hg emissions (Fu et al., 2011a; Zhu et al., 2012; Chen et al., 2013). For example, previous studies estimated that annual anthropogenic Hg emissions in Guiyang and Nanjing over the last few years reached 1.75 and 4.26 t, respectively (Zhu et al., 2012; Fu and Feng, 2015). Large emissions of Hg from natural surfaces in the urban areas of China may also play a role for the elevated GEM concentrations (Feng et al., 2005; Wang et al., 2006a; Zhu et al., 2012). There is a clear spatial distribution pattern of GEM, with relatively higher values in inland cities and lower values in coastal cities due to the influence of the clean marine air (Fig. 1). The average GEM concentrations in coastal cities including Qingdao, Shanghai, Ningbo, Xiamen, and Guangzhou were in the range of 2.70–4.6 ng m^{-3}, which were significantly lower than that (6.74 to 28.6 ng m^{-3}) in inland cities.

3.1.2 Total particulate bounded mercury (TPM) and fine particulate bounded mercury (PBM)

TPM/PBM concentrations at remote and urban sites of China ranged from 18.9 to 154 pg m^{-3} (mean = 51.8 pg m^{-3}, n = 8) and from 141 to 1180 pg m^{-3} (mean = 530 pg m^{-3}, n = 9), respectively. These are significantly higher (several to dozens of times) than the observations in North America and Europe (Table 1). The highest TPM concentration (1180 ± 820 pg m^{-3}) in urban areas was observed in Beijing. The highest PBM concentration (154 ± 104 pg m^{-3}) at remote sites was observed at Mt. Damei Observatory, a mountain site located in the Yangtze River Delta, one of most industri-

ACPD
15, 11925–11983, 2015

alized and urbanized regions in eastern China. The elevated TPM/PBM concentrations in urban areas were most likely due to anthropogenic emissions (Wang et al., 2006b; Xiu et al., 2005; Fu et al., 2011a) that can undergo regional transport and influence atmospheric Hg level at the remote sites (Zhang et al., 2013). A positive correlation exists between PBM and GEM concentrations observed at remote sites in China (Fig. 3), indicating PBM and GEM may share common emission sources. The size-fractionation of particulate Hg in urban areas of China has been investigated. The studies in Beijing, Nanjing, and coastal cities of southeast China revealed that PBM (the fraction associated with particles having a diameter of $< 2.5\,\mu m$) constituted 40–70 % of the TPM. Given that fine particles are removed from atmosphere less efficiently than the large particles (Zhang et al., 2001), the fraction of PBM in TPM is likely higher in remote areas than in urban areas.

TPM/PBM makes up an important fraction of atmospheric Hg in the urban areas of China. Average TPM/GEM concentration ratios in Beijing, Nanjing, Shanghai, Qingdao in northern and eastern China ranged from 8.8 to 20.7 %, much higher than the PBM/TGM ratio of 3.8–5.0 % in Guiyang, southwest China and Xiamen, southeast China (Table 1). Average PBM/GEM ratios at remote sites (1.0–4.6 %) are lower than that in urban areas. The two highest PBM/GEM ratios among the remote sites were observed at Mt. Damei (5.4 %) and Miyun (3.0 %), both are located near urban areas (Fig. 3). PBM/GEM ratios (1.0–1.5 %) at remote sites in northeast, northwest, and southwest China are much lower. This is consistent with the spatial distribution pattern of anthropogenic Hg emissions and particulate pollution in China (van Donkelaar et al., 2010; AMAP/UNEP, 2013). TPM/PBM is more readily removed from the atmosphere than GEM. Therefore, the concentration ratios between TPM/PBM and GEM are expected to be higher at sites near anthropogenic source regions. In addition, formation of TPM via adsorption of gaseous mercury on to airborne particles may be also important (Zhu et al., 2014). The ratios of TPM to total Hg from anthropogenic emissions are < 5 % (Streets et al., 2005), significantly lower than the observed ratios in some urban areas in northern and eastern China.

ACPD
15, 11925–11983, 2015

3.1.3 Gaseous oxidized mercury (GOM)

Measurements of GOM concentrations in urban areas have been conducted in Guiyang, southwest China and Xiamen, southeast China. The mean concentrations of GOM in Guiyang and Xiamen were 35.7 ± 43.9 and $61.0 \pm 69.0\,pg\,m^{-3}$, respectively (Table 1), higher than most of the observations in urban areas of North America and Europe (typically $< 15\,pg\,m^{-3}$), with the exception of St. Louis, Illinois, central USA (GOM mean $= 37.2\,pg\,m^{-3}$) and Reno, Nevada, western USA (GOM mean $= 26.0\,pg\,m^{-3}$) (Peterson et al., 2009; Engle et al., 2010). The former was heavily impacted by nearby sources and the latter was influenced by in-situ production and mixing of GOM from free troposphere (Peterson et al., 2009; Engle et al., 2010). In Chinese cities, anthropogenic emission is the dominant factor attributing to the elevated GOM concentrations. The study in Guiyang found that many spikes of GOM concentrations were associated with plumes from large point sources including a coal-fired power plant and a cement factory.

Average GOM concentrations at the 7 remote sites of China ranged from 2.2 to $10.1\,pg\,m^{-3}$ (mean $= 6.6 \pm 2.4\,pg\,m^{-3}$), only slightly higher than those observed from North America and lower than those in Europe (Table 1). GOM concentrations at 9 remote sites in central and eastern USA were in the range of 0.4–$6.6\,pg\,m^{-3}$ (mean $= 2.5 \pm 2.4\,pg\,m^{-3}$) (Lan et al., 2012). Sources of GOM at remote sites include local anthropogenic emissions, regional transport from urban and industrial areas, in-situ photochemical production and intrusion of GOM-enriched air from the free troposphere. At the remote sites in eastern and northern China, the local sources (such as domestic heating in small settlements) located within 10 km from the sites may be responsible for the elevated GOM concentrations. The impact of long-range transport from industrial and urbanized areas is rare because of the fast deposition of GOM. However, under certain air conditions such as low air humidity and high wind speed, the possibility of regional transport of GOM may not be ruled out. For example, the observations at Mt. Waliguan, northeast Tibetan Plateau found many of high-GOM events were related to

ACPD
15, 11925–11983, 2015

air plumes originated from industrial and urbanized centers that are about 90 km to the east of the sampling site (Fu et al., 2012a). In-situ production is also an important source of GOM at remote sites. Several studies observed a remarkable diurnal pattern for GOM with relatively higher concentrations during daytime that cannot be explained by emissions (Fu et al., 2012a; Zhang et al., 2013). Although not as significant as in the polar region, free troposphere and marine boundary layer (Lindberg et al., 2002; Swartzendruber et al., 2006; Timonen et al., 2013), in-situ GOM production is an important source of GOM in remote areas of China. There are currently no evidences with respect to the mixing of GOM-enriched air from the upper troposphere/lower stratosphere being observed in China, mainly because most of the sampling sites are located in low-altitude areas or the local topography does not favor the intrusions of air massed from the upper troposphere/lower stratosphere.

3.2 Atmospheric mercury in marine boundary layer

The first measurement of GEM in the Chinese marine boundary layer was made on board of a ship during a cruise campaign in the northern South China Sea (SCS) in August 2007 (Fu et al., 2010c). The northern SCS is surrounded by several counties including China, Vietnam and Laos in the Indo-China Peninsula, and Philippines. GEM concentration in the marine boundary layer displayed a clear spatial distribution pattern in the northern SCS with concentrations (1.29–1.94 $ng\,m^{-3}$) close to the background values (1.5–1.7 $ng\,m^{-3}$) in the Northern Hemisphere and with elevated concentrations (2.5–4.71 $ng\,m^{-3}$) measured at sites close to mainland China (Fig. 4). Backward trajectory analysis indicated that most of the high-GEM events were related to air masses originated from southern China and Indo-China Peninsula (Fu et al., 2010c). These results suggest that the southern China and Indo-China Peninsula are important source regions of atmospheric Hg and have strong impacts on atmospheric Hg pollution in the North SCS. Atmospheric Hg emissions from mainland China have been well investigated (Streets et al., 2005; Wu et al., 2006; Shetty et al., 2008). However, there is a lack of information regarding Hg emissions in the Indo-China Peninsula. An ex-

ACPD
15, 11925–11983, 2015

periment study in Da Nang, central eastern Vietnam reported a mean GEM concentration of 3.86 ng m^{-3}, more than 2 times higher than the background values in the Northern Hemisphere. This indicates significant anthropogenic emissions of Hg in the Indo-China Peninsula (Sheu et al., 2013). The outflow of Hg from mainland China and Indo-China Peninsula to the SCS is expected to vary with the monsoon (Fu et al., 2010c). The cruise measurements by Fu et al. (2010c) were conducted in summer and the observations in the open sea was less impacted by outflows of Hg from mainland China and Indo-China Peninsula because of the predominant southeast monsoon. However, as the northwest monsoon becomes predominant in winter and spring, the impact of Hg emissions in mainland China and Indo-China Peninsula on atmospheric pollution in the SCS is expected to increase. This was verified by the seasonal observations of GEM at Dongsha Island in the open sea of SCS, which reported that mean GEM concentration in spring (March–April 2008) was 56 % higher than that in summer (August 2008) (Sheu et al., 2013).

GEM in the marine boundary layer has been investigated in the Bohai Sea and Yellow Sea. Ci et al. (2011b) performed a cruise campaigns over the Yellow Sea and Bohai Sea from 9 to 18 July 2010, and showed an average GEM concentration of 2.61 ± 0.50 ng m^{-3}, comparable with the mean value obtained from the northern SCS (Fu et al., 2010c) and significantly higher than those measured in the Atlantic Ocean, North Sea, Baltic sea, Adriatic Sea, and Mediterranean Sea (Leermakers et al., 1997; Wangberg et al., 2001; Temme et al., 2003; Gardfeldt et al., 2003; Sprovieri and Pirrone, 2008). An apparent spatial distribution pattern of GEM concentrations showed elevated concentrations at sites close to Chinese coast and lower concentrations in the eastern Bohai Sea and Yellow Sea (Ci et al., 2011b). The GEM also varied with the sources of air masses. Elevated GEM concentrations were mostly related to the outflows from mainland China, indicating a strong impact of anthropogenic Hg emissions in coastal and open sea areas of China (Ci et al., 2011b). Cruise measurements of GEM concentrations in marine boundary layer of Yellow Sea were made by Nguyen et al. (2011). The results revealed that GEM concentrations were relatively higher in

ACPD
15, 11925–11983, 2015

the Yellow Sea (range from 1.50 to 2.50 ng m^{-3}) than in the western coast of Korea (range from 1.40 to 2.00 ng m^{-3}) (Nguyen et al., 2011). GEM concentrations in marine boundary layer of the East China Sea (ECS) were measured on board during the cruise campaign from Shanghai, China to Antarctic (Xia et al., 2010). This study navigated the east of ECS and showed a mean value of 2.32 ± 0.49 ng m^{-3} in the ECS, and coast of Japan and Korea (Xia et al., 2010).

3.3 Atmospheric mercury in the free troposphere and lower stratosphere

GEM concentrations in the upper troposphere/lower stratosphere (10–12 km a.s.l.) over mainland China were measured onboard a passenger aircraft during dozens of CARIBIC flights from Frankfurt, Germany to Guangzhou, China (Slemr et al., 2009; Lai et al., 2011). Slemr et al. (2009) depicted the time-longitude distribution of upper tropospheric GEM concentrations crossed northwest China and southern coastal China. The GEM concentrations in upper troposphere/lower stratosphere over mainland China were in the range of 0.5–1.5 ng m^{-3} for most cases with the exception in the proximity of Guangzhou, southern China, which showed GEM concentrations exceeding 2.0 ng m^{-3}. Stratospheric measurements of GEM were also made over the South China Sea (SCS) during the flight from Guangzhou, China to Manila, Philippines (Lai et al., 2011). The GEM concentrations in the upper troposphere/lower stratosphere over the SCS were in the range of 0.8–1.8 ng m^{-3}, comparable with that over the mainland China. The levels of GEM in the upper troposphere/lower stratosphere over China are comparable with the observations over southern Europe, western Africa, Atlantic Ocean, and western South America (Slemr et al., 2009) as well as North America and North Pacific Ocean (Talbot et al., 2007; Lyman and Jaffe, 2012). Ozone concentrations in the upper troposphere/lower stratosphere are up to 1000 ppb and can facilitate the fast depletion of GEM (Slemr et al., 2009; Lyman and Jaffe, 2012). Also, the upper troposphere/lower stratosphere has high horizontal wind speed and weak mixing of air from lower troposphere. Hence, GEM concentrations measured in the upper tro-

ACPD
15, 11925–11983, 2015

posphere/lower stratosphere over China were more likely to represent an overall level of atmospheric GEM in the upper troposphere/lower stratosphere in continental and/or hemispheric scale.

Nevertheless, several high-GEM events in the upper troposphere/lower stratosphere over mainland China were observed (Slemr et al., 2009). These events were accompanied by elevated CO, aerosols, NOy, and CH_3CN concentrations. Backward trajectories analysis suggested air masses during these events were originated from planetary boundary layer over southern China (Slemr et al., 2009). Lai et al. (2011) studied a specific event over southern China in July 2007. The GEM concentrations in the upper troposphere/lower stratosphere during the event ranged from 2.0 to 4.0 $ng\,m^{-3}$, much higher than the rest of observations. This event was impacted by anthropogenic sources in southern China via strong convective processes (Lai et al., 2011). The impact of emissions in mainland China on GEM in the free troposphere was also detected during the flights over East Asia (Friedli et al., 2004). The flight measurements observed several strong GEM pollution events with concentrations exceeding 2.5 $ng\,m^{-3}$ (up to 6.3 $ng\,m^{-3}$), which were caused by encounters of polluted air plumes from eastern China (Friedli et al., 2004).

3.4 Seasonal variations of atmospheric mercury

Figure 5 shows the seasonal variations of GEM concentrations at Chinese ground-based remote sites. All observations showed strong seasonal variations in GEM concentrations. The variations can be classified into two distinct types. The first showed the maximum in winter and minimum in summer, such as at the sites of Mt. Gongga, Mt. Damei, Mt. Leigong, and Mt. Changbai (Fig. 5). The most pronounced seasonal pattern was observed at Mt. Gongga and Mt. Leigong, with the mean concentrations in winter about 2 times higher than that in summer (Fu et al., 2008b, 2010b). The second seasonal pattern exhibits the maximum in summer and minimum in winter, which includes the observations at Miyun, Mt. Waliguan and Mt. Ailao (Fig. 5). Seasonal patterns of GEM concentrations in urban areas of China were also different among sites.

ACPD
15, 11925–11983, 2015

In Guiyang, southwest China, GEM concentrations were highest in winter and lowest in summer (Feng et al., 2004). The seasonal pattern of GEM in Nanjing, eastern China was in contrast to that in Guiyang, southwest China, with the summer mean concentration ~ 2 folds higher than that in winter (Zhu et al., 2012). The study in Guangzhou, southern China showed the lowest mean value in summer, which is similar to Guiyang, but its maximum mean concentration was observed in spring (Chen et al., 2013).

There are several causes regulating the seasonal variations of GEM in China. Seasonal changes in anthropogenic Hg emissions related to coal and biofuel combustion in urban and residential heating were suggested to be important (Feng et al., 2004; Fu et al., 2008b, 2010b). According to the statistical data of energy consumption in China in 2011 (National Bureau of Statistics of China, 2012), annual coal consumption for urban and residential heating reached 168 million and 92 million t, respectively, accounting for about 7.5 % of the total coal consumption in China. Coal combustion in these heating systems mainly occurred in winter and lacked emission control devices (Pacyna et al., 2010; Pirrone et al., 2010), which may release significant amount of atmospheric Hg and consequently influence the seasonal trend of GEM in many regions of China (particularly in regions with a cold winter climate). GEM (Hg^0) emission from natural surfaces was also reported to be responsible for seasonal trend of GEM (Zhu et al., 2012). GEM emission fluxes from natural surfaces are generally influenced by meteorological parameters such as solar radiation and air temperature and exhibited strong seasonal variations with increasing emission fluxes in summer (Wang et al., 2004; Fu et al., 2008a, 2013). The study in Nanjing found that GEM concentrations were strongly positively correlated with air temperature and solar radiation, indicating natural emissions made a significant contribution to the elevated GEM concentrations in summer (Zhu et al., 2012). Monsoon dominated long-range transport was another reason for the seasonal trends of GEM in China. The northerly winter monsoon (northwest monsoon) and East Asian summer monsoon (including southwest and southeast monsoon) are the two predominant monsoons that influence the prevailing winds in East Asia (An, 2000). As shown in Fig. 6, the summer wind flows in eastern China

ACPD
15, 11925–11983, 2015

are mainly originated from India Ocean and western Pacific Ocean and move northwards from southwest and southeast China to northern China, while the winter wind flows are mainly originated from Siberia and move southwards from northern China to southeast. Given the pronounced spatial pattern of anthropogenic Hg emissions in China and East Asia (Fig. 2), the circulation of the monsoons could change the source-receptor relationships at most of the monitoring stations and influences the seasonal trend of GEM concentrations. For example, the elevated GEM concentrations in summer at Mt. Waliguan, northwest China and Miyun, northern China, both under the influence of East Asian summer monsoon, were attributed to the long-range transport of GEM from source areas to the east and south of the two sampling sites, respectively (Fu et al., 2012a; Zhang et al., 2013). Zhang et al. (2015a) proposed that long-range transport of GEM-enriched air masses from South Asia, which was caused by the southwest monsoon (Indian summer monsoon) and westerlies, played an important role in the elevation of GEM concentration at Shangri-La, southwest China in spring. Other processes such as changes in atmospheric photochemical processes, dry deposition, mixing layer depth, and meteorological conditions may also be responsible for the seasonal trend of GEM in China (Fu et al., 2008b, 2012b; Chen et al., 2013).

Seasonal variations of atmospheric TPM/PBM have also been reported. Most reports showed a lower average concentration of TPM/PBM in summer, while the higher mean concentration (up to one order of magnitude higher than in summer) was observed both in winter (Wang et al., 2006b; Fu et al., 2008c; Zhu et al., 2014) and autumn (Zhang et al., 2013; Xu et al., 2013; Zhang et al., 2015a). The high levels of TPM/PBM in winter and autumn coincided with the particulate pollution during these periods, which was likely caused by direct anthropogenic particulate mercury emissions and formation of secondary particulate mercury via gas-particle partitioning processes (Wang et al., 2006b; Fu et al., 2008c; Zhu et al., 2014). Seasonal variations of GOM concentrations were not extensively studied in China. The studies at Mt. Gongga, southwest China and Miyun, northern China showed the GOM concentrations were lower in winter and higher in spring and autumn, in contrast with the seasonal patterns

ACPD
15, 11925–11983, 2015

of GEM and TPM/PBM (Fu et al., 2008c; Zhang et al., 2013). Explanations for the seasonal trend of GOM include stronger gas-particle partitioning of GOM at lower air temperature and higher particulate concentrations in winter, as well as faster photochemical productions of GOM in warm seasons (Fu et al., 2008c; Zhang et al., 2013).

3.5 Diurnal variations of atmospheric mercury

Figure 7 displays the diurnal variations of GEM observed at the remote sites of China. Most of the observations showed a well-defined diurnal trend with elevated concentrations during daytime and lower values at night, with the exceptions at Mt. Waliguan and Miyun. This diurnal pattern highlights the impact of regional anthropogenic Hg emissions. Most of the remote sampling sites in China were located at a relatively high altitude and regional anthropogenic sources are distributed in low-altitude areas surrounding the monitoring sites. These sites were influenced by the diurnal alternations of mountain valley breezes which bring Hg-polluted air to the sampling sites during daytime (Fu et al., 2008b, 2010b; Chen et al., 2013). Also, dry deposition of GEM to forest canopy during the buildup of nocturnal boundary layer was of specific importance for decreased nighttime GEM concentrations at a forest site in Mt. Changbai, northeast China (Fu et al., 2012b). The diurnal pattern of GEM at Mt. Waliguan and Miyun was in contrast with those observed in other remote sites (Fig. 6). The elevated concentrations during nighttime at Mt. Waliguan were mainly related to downward intrusion of free troposphere airflow originated from industrialized and urbanized areas via long-range transport (Fu et al., 2012a).

Diurnal trend of GEM in urban areas of China have been investigated in Guiyang, Nanjing, Hefei, Xiamen, and Guangzhou (Feng et al., 2004; Zhu et al., 2012; Chen et al., 2013; Li, 2012; Xu et al., 2015). The diurnal trends of GEM in Guiyang, Hefei, Xiamen and Guangzhou were similar, with relatively higher concentrations observed at night. This was mainly due to the accumulation of Hg emitted from local sources in the shallow nocturnal boundary layer (Feng et al., 2004; Chen et al., 2013; Li, 2012). The diurnal trend of GEM in Nanjing was different. It exhibited higher concentrations

ACPD
15, 11925–11983, 2015

from early morning to noon, which was attributable to natural emissions and downward mixing of air masses from aloft (Zhu et al., 2012).

Several studies have investigated the diurnal variations of PBM and GOM in China (Fu et al., 2008c, 2011a, 2012a; Zhang et al., 2013). In Guiyang, Mt. Waliguan, and Miyun, elevated PBM concentrations were observed at night. The most pronounced diurnal variation of PBM was observed in Guiyang, with the peak hourly-averaged PBM concentration observed at night and about 9 times higher than the minimum observed during daytime, suggesting the impact of local PBM emissions during the buildup of nocturnal boundary layer (Fu et al., 2011a). The elevated PBM at night at Miyun was related to the formation of temperature inverse layer (Zhang et al., 2013), while that at Mt. Waliguan were caused by long-range transport (Fu et al., 2012a).

All GOM measurements in the remote and urban areas of China displayed a well-defined diurnal trend with increasing concentrations during daytime, coinciding with increasing solar radiation and atmospheric oxidants concentrations (Fu et al., 2008c, 2011a; Zhang et al., 2013, 2015a). The diurnal trend of GOM is more pronounced at remote sites where the impact of anthropogenic emissions was minimal and in warm seasons when levels of atmospheric oxidants and solar radiation were high (Fu et al., 2008c; Zhang et al., 2013). This result is consistent with the observations in North America and Europe (Munthe et al., 2003; Lan et al., 2012). Both anthropogenic sources and photochemical oxidation can produce atmospheric GOM. Photochemical oxidation produces approximately 8000–15 000 t of atmospheric GOM annually (Selin et al., 2007; Driscoll et al., 2013), about 10–20 times higher than the emissions from anthropogenic sources. Although previous studies demonstrated that this process mainly occurred in the free troposphere, stratosphere, polar regions, and marine boundary layer (Lindberg et al., 2002; Swartzendruber et al., 2006; Fain et al., 2009; Lyman and Jaffe, 2012; Timonen et al., 2013), the well-defined diurnal pattern of GOM at remote sites in China suggests that the photochemical oxidation may also play an important role in the formation of GOM in continental boundary layer.

ACPD
15, 11925–11983, 2015

3.6 Long-term trend of atmospheric mercury distribution in ambient air

Long-term trend of GEM in South Africa, Europe, and North America have been well documented (Slemr and Scheel, 1998; Slemr et al., 2003, 2011; Ebinghaus et al., 2002; Cole et al., 2013). These trends showed slowly decreasing GEM concentrations over the past two decades. Slemr et al. (2011) observed that GEM concentrations decreased from $\sim 1.35\,ng\,m^{-3}$ in 1996 to $\sim 0.9\,ng\,m^{-3}$ in 2008 in South Hemisphere and from $\sim 1.75\,ng\,m^{-3}$ in 1996 to $\sim 1.4\,ng\,m^{-3}$ in 2009 at Mace Head, Europe, corresponding to annual decreasing rates of 0.024–0.035 $ng\,m^{-3}\,yr^{-1}$. The ten-year trends of GEM concentrations at five ground-based sites in the Arctic and Canada also showed a decreasing trend with annual decreasing rates ranging of 0.013–0.035 $ng\,m^{-3}\,yr^{-1}$ (0.9–2.2 $\%\,yr^{-1}$) (Cole et al., 2013). Such a decrease is consistent with the temporal trends of anthropogenic mercury emissions in Europe and North America but contrary to the temporal trends of global anthropogenic mercury emissions (Pirrone et al., 1996; Pacyna et al., 2003; AMAP/UNEP, 2013; Muntean et al., 2014).

Knowledge of long-term trend of GEM in China is currently scarce. However, several preliminary studies have been carried out and may provide clues in the long-term trend of GEM in China. For example, Fu and Feng (2015) found that the annual mean GEM concentration in Guiyang, southwest China increased from $8.40\,ng\,m^{-3}$ (geomean $= 7.46\,ng\,m^{-3}$) around 2002 to $10.2\,ng\,m^{-3}$ (geomean $= 8.88\,ng\,m^{-3}$) around 2010. Assuming a constant GEM increasing rate during 2002–2010, the mean annual increasing rate can be estimated to be $0.16\,ng\,m^{-3}\,yr^{-1}$ ($2.5\,\%\,yr^{-1}$). The increase of GEM in Guiyang was mainly observed during cold season and daytime (Fig. 8), when the impact of regional emissions and long-range transport from central China played a more important role. The annual mean GEM concentration at Mt. Changbai, northeast China around 2014 was reported to be $1.73\,ng\,m^{-3}$, which was $0.17\,ng\,m^{-3}$ higher than that observed around 2009 (Fu et al., 2012b). This corresponded to a mean annual increasing rate of $0.034\,ng\,m^{-3}\,yr^{-1}$ ($2.1\,\%\,yr^{-1}$). These observations implied that the levels of GEM may undergo a slight increase in some regions of China. This as-

ACPD
15, 11925–11983, 2015

sessment is apparently consistent with the recent Chinese anthropogenic Hg emission inventories that showed increasing anthropogenic Hg emissions due to the increasing consumption of resources and productions of mercury-containing products (Wu et al., 2006; Pacyna et al., 2010; Liang et al., 2013). Nevertheless, it should be noted that the above measurements were based on two separated year of continuous measurements. Also, the limited data seems insufficient to depict the overall trend of GEM in China as the temporal trend in Hg emission strength may not be the same for different regions in China. Therefore, the above assessment may have large uncertainties. However, long-term continuous measurements of atmospheric GEM is ongoing at several remote sites in China. These works will help to better understand the long-term trend of atmospheric GEM in China and the response of atmospheric Hg to anthropogenic Hg emissions.

3.7 Implications of mercury emissions in China

Field measurements of atmospheric Hg are useful for constraining atmospheric Hg emissions. A previous study by Pan et al. (2007) used an inverse modeling method combined with the assimilation of aircraft measurements of atmospheric Hg in East Asia to estimate Hg emissions in China. It suggested that a total annual Hg^0 (GEM) emission of 1140 t in China could make model predictions better match the field observations of atmospheric Hg, which is about 3.4 times higher than the total anthropogenic Hg^0 (GEM) emissions (340 t) in China for 1999. Later, a CMAQ-Hg modeling approach was utilized to predict the ground-based concentrations of atmospheric Hg in East Asia (Lin et al., 2010). This study predicted concentrations of atmospheric Hg using a base case (a total Hg emission of 1793 t in East Asia) and an inferred case (a total Hg emission of 2258 t in East Asia) of emission scenarios. The results revealed that the model-predicted concentrations at remote sites were consistent with field observations but that in urban areas were significantly lower than filed observations at urban sites in China. The discrepancy between model-predicted and observed concentrations was likely due to the underestimate of Hg emissions and missing of certain emission

ACPD
15, 11925–11983, 2015

sources (Lin et al., 2010). Recently, Wang et al. (2014a) applied a GEOS-Chem model using the total Hg emission of 1921 t in East Asia (966 t from anthropogenic sources and 955 t from natural sources) to simulate atmospheric Hg concentrations and depositions in China. The simulated concentrations of atmospheric Hg were in a good agreement with observed concentrations.

Estimates of Hg^0 emissions in China have also been made using a correlation analysis between observed GEM and trace gases concentrations. This approach based on measured ratios of GEM to trace gases in plumes originated from China and verified inventories of trace gases in China. Table 2 summarized the observed GEM/CO ratios in China reported by a number of previous studies. The average GEM/CO ratios in China were in the range of 2.6–11.4 $pg\,m^{-3}\,ppb^{-1}$. The variations in GEM/CO ratios were likely attributed to the impact of different emissions sources in China which may have distinct emission ratios of GEM/CO (Fu et al., 2015). Using the GEM/CO ratios reported from different regions of China, we calculated the overall mean GEM/CO ratio in China to be 6.7 ± 2.8 ($n = 12$) pg $m^{-3}\,ppb^{-1}$. Given the latest estimate of annual total CO emissions of 183×10^6 t in China (Zhao et al., 2012), annual total GEM emissions in China was estimated to be 983 t in 2009. This value is significantly higher than the anthropogenic GEM emissions (318–395 $t\,yr^{-1}$) in China (Wu et al., 2006; AMAP/UNEP, 2013; Wang et al., 2014a). Underestimates of anthropogenic Hg emissions in China were supposed to be an important reason contributing to the discrepancy between modeled Hg^0 emissions and anthropogenic emission inventories (Jaffe et al., 2005; Weiss-Penzias et al., 2007; Fu et al., 2015). Advances in field measurements of Hg emission factors for large point emission sources have significantly reduced the uncertainties of Hg emission inventories of industrial point sources (Wang et al., 2014b). However, knowledge gaps still remain in emission estimates of several categories in China. China is the largest producer (1300–1500 $t\,yr^{-1}$) and consumer ($\sim$ 1000 $t\,yr^{-1}$) of Hg worldwide (USGS, 2014). Hg emissions related to the production, consumption and recycling of Hg in artisanal mercury and gold productions, polyvinyl chloride (PVC) production, mercury batteries, mercury sphygmomanometer, and mercury thermome-

ACPD
15, 11925–11983, 2015

ter were not well understood (Li et al., 2009; Ren et al., 2014). The emissions from these sections may be important contributors to the anthropogenic Hg emissions in China. Other potential mechanisms including natural emissions and conversion of Hg species and trace gases during long-range transport should be also evaluated to better constrain Hg emissions of China (Jaffe et al., 2005).

3.8 Long-range transport of atmospheric mercury

Most anthropogenic Hg emissions in China are related to domestic industrial and urban sources (Wang et al., 2014a). Strong Hg emissions in urban areas not only result in highly elevated GEM concentrations locally, but also impact the GEM levels in remote areas via long-range transport. Figure 8 shows the potential source regions of GEM at Mt. Waliguan, northwest China, Mt. Changbai, northeast China, Mt. Leigong, southwest China, and Mt. Damei, eastern China obtained by the Potential Source Contribution Function (PSCF) analysis. The source regions of Mt. Waliguan were mainly related to industrialized and urbanized areas in northwest China which are 100–400 km to the east of the sampling site as well as northern India (Fu et al., 2012a). For Mt. Changbai, northern China where many megacities such as Beijing, Tianjin, and Shijiazhuang are located was identified as potential source regions (Fu et al., 2012b). The identified source regions of Mt. Changbai were more or less similar to that of Miyun, northern China (Zhang et al., 2013). The source regions of Mt. Leigong included a megalopolis in southwest China (including Chongqing, Guiyang, and Kunming, with a population of ~20 million), as well as the northern Myanmar, in which forest biomass burning released huge air pollutants to the atmosphere (Streets et al., 2003). The source regions of GEM at Mt. Damei were mainly central Anhui province and western Jiangshu province, both being important industrial region in eastern China (Yu et al., 2015). The identified source regions corresponded reasonably to the distributions of anthropogenic Hg sources in China and other Asian countries (Fig. 2). Long-range transport of atmospheric Hg from major anthropogenic Hg source regions in East Asia played an important role in the elevated GEM concentrations at remote sites in China. These

ACPD
15, 11925–11983, 2015

studies also elucidated that the dominant transport routes of atmospheric Hg in China, such as from northwest to the Tibetan Plateau, from northern China to northeast China, from southwest to central China, and from eastern China to coastal areas of eastern China and East China Sea, are likely related to dominant wind directions in East Asia governed by the monsoon. On the other hand, long-range transport played a minor role in urban areas of China (Fu et al., 2011a; Zhu et al., 2012) mainly because of the predominant local anthropogenic sources that elevated GEM concentrations in urban areas.

Due to the elevated atmospheric Hg concentrations, air flows from mainland China may also impact the atmospheric Hg pollutions in other countries and regions. For instance, the measurements of atmospheric GEM in Seoul, Korea found that approximately 79 % of the high GEM events were related to air flows originated from mainland China (Choi et al., 2009). Also, flight measurements in free troposphere over Asia Pacific region encountered several industrial plumes from east China coast which elevated atmospheric GEM levels by a factor of 2–4 (Friedli et al., 2004). Hg emitted in mainland China can also undergo transcontinental transport. Such a long-range transport has been investigated at Mount Bachelor Observatory (MBO) in the Pacific Northwest of USA (Jaffe et al., 2005; Weiss-Penzias et al., 2006; Strode et al., 2008; Timonen et al., 2013). The trans-Pacific transport of Hg from mainland China (possibly including other East Asia countries) mainly occurred in spring and was reported to result in a 10–40 % increase of GEM at MBO (Jaffe et al., 2005; Weiss-Penzias et al., 2006).

3.9 Atmospheric mercury depositions in China

Previous measurements of THg and MeHg concentrations as well as deposition via precipitation, throughfall, and litterfall in China are presented in Table 3. Average THg and MeHg concentrations in wet-only precipitation at remote sites ranged from 3.0 to 4.8 ng L^{-1} (mean = 4.0 ng L^{-1}, $n = 4$) and from 0.03–0.04 ng L^{-1} (mean = 0.04 ng L^{-1}, $n = 2$), respectively. THg and MeHg concentrations in wet-only precipitation were much higher in urban areas, with the mean values in the ranges of 13.3–52.9 ng L^{-1} (mean

ACPD
15, 11925–11983, 2015

= 31.2 ng L^{-1}, n = 5) and 0.05–0.31 ng L^{-1} (mean = 0.18 ng L^{-1}, n = 2), respectively. It is worth noting that THg and MeHg concentrations in bulk precipitation at remote sites of China were much higher than that of wet-only precipitation (Table 3). Some of the bulk precipitation samples were collected at locations close to anthropogenic Hg sources and on a monthly basis (Guo et al., 2008; Fu et al., 2008c; Wan et al., 2009b), which might incorporate dry deposition of Hg and overestimate wet deposition of Hg. Wet-only deposition fluxes of THg and MeHg at remotes sites of China were 1.8–7.0 μg m^{-2} yr^{-1} (mean = 5.1 μg m^{-2} yr^{-1}, n = 4) and 0.01–0.06 μg m^{-2} yr^{-1} (mean = 0.04 μg m^{-2} yr^{-1}, n = 2), respectively, and they were 13.4–56.5 μg m^{-2} yr^{-1} (mean = 31.9 μg m^{-2} yr^{-1}, n = 4) and 0.05–0.28 μg m^{-2} yr^{-1} (mean = 0.16 μg m^{-2} yr^{-1}, n = 2) in urban areas, respectively (Table 3). Wet deposition fluxes of THg and MeHg in urban areas of China were relatively higher compared to those in North America and Europe (Table 3). This is consistent with the elevated GEM, PBM, and GOM in urban areas of China. However, wet deposition fluxes of THg and MeHg at remote sites of China were within the lower range of that in North America and Europe (Table 3). This is in contrast with the elevated GEM and PBM concentrations at remote sites of China. This indicates that atmospheric Hg in the boundary layer (related to scavenging processes below cloud) is not the exclusive source of Hg in precipitation at remote sites in China, while global and/or continental transport of cloud water and levels of atmospheric PBM and GOM in the free troposphere and stratosphere could play a significant role (Dastoor and Larocque, 2004).

Dry deposition fluxes of Hg, calculated on basis of subtracting wet deposition in open areas from the sum of loadings in throughfall and litterfall, were measured at several forest sites in China (Graydon et al., 2008). Mean dry deposition fluxes of THg at Mt. Gongga and Mt. Leigong, both being remote sites in southwest China, were in the range of 43.9–66.5 μg m^{-2} yr^{-1} (mean = 55.2 μg m^{-2} yr^{-1}, n = 2) (Fu et al., 2010a, b). Dry deposition flux of Hg near Chongqing, southwest China showed a mean flux of 262 μg m^{-2} yr^{-1} (Wang et al., 2009). Dry deposition fluxes of Hg at forest sites in China were elevated by a factor of 1.8–13.6 compared to those observed in North

ACPD
15, 11925–11983, 2015

America (range: 13.3–34.0 $\mu g\,m^{-2}\,yr^{-1}$, mean = 19.2 $\mu g\,m^{-2}\,yr^{-1}$, $n = 5$) and Europe (range: 25.3–36.0 $\mu g\,m^{-2}\,yr^{-1}$, mean = 29.6 $\mu g\,m^{-2}\,yr^{-1}$, $n = 5$) (Lee et al., 2000; Grigal et al., 2000; Rea et al., 2001; St Louis et al., 2001; Lindberg et al., 2007).

Dry deposition fluxes of Hg were significantly higher than that of wet deposition fluxes of Hg in forest areas of China. For instance, dry deposition fluxes of Hg at Mt. Gongga and Mt. Leigong in southwest China were approximately 2.5 and 7.2 times higher than the wet deposition fluxes, respectively (Fu et al., 2010b, a).The mean ratio of dry deposition fluxes to wet deposition fluxes in Tieshanping, Chongqing, which was close to anthropogenic sources, was up to 9 (Wang et al., 2009). This is consistent with the results predicted by modeling studies, although the measured ratios were significantly higher than modeling results in China (Lin et al., 2010; Wang et al., 2014a). This highlights the role of forest in the cycling of atmospheric Hg in China.

4 Conclusions

As the largest atmospheric mercury source region in the world, much attention has been paid to the atmospheric Hg pollution in China. This paper provides a comprehensive review on the atmospheric Hg studies in China. All atmospheric Hg species in remote and urban areas of China were found to be elevated compared to those in North America and Europe. This reflects that China is a strong source region of atmospheric Hg. Estimates of Hg emissions based on correlation slopes between GEM and CO concentrations suggested that China released about 983 t of GEM to the atmosphere annually. This agrees well with the modeling assessment but much higher the published anthropogenic GEM emission inventories that might have underestimated the true emission values due to the unaccounted anthropogenic and natural sources. Field measurements showed a clear increasing trend of GEM concentrations in China over the past decade, suggesting increasing anthropogenic emissions related to growing consumption of resources and productions of mercury-containing products. The seasonal and diurnal variations of GEM, PBM, and GOM were apparent in most obser-

ACPD
15, 11925–11983, 2015

vations, but the trends were different at the monitoring sites, indicating the combined effect of the local and regional emissions, natural emissions, monsoon dominated long-range transport as well as atmospheric photochemical processes, dry deposition, and meteorological conditions. The THg concentrations and deposition fluxes of wet-only precipitation in the remote areas of China were slightly lower than those in North America and Europe. This is in contrast to the high anthropogenic Hg emissions and atmospheric Hg concentrations in China, suggesting that domestic Hg pollution in China may not be the exclusive factor influencing atmospheric wet deposition of Hg in remote areas. On the other hand, dry depiction of Hg especially in forest areas of China were highly elevated compared to the observations in North America and Europe. This implies that uptake of atmospheric Hg by vegetation foliar could be an important sink of atmospheric Hg in China.

Although many advances have been achieved over the past two decades, more studies are needed to improve our understanding on the fate of atmospheric Hg in China and the roles of China emissions in global Hg cycling. Future studies should focus on the several areas:

- A coordinated national monitoring network of atmospheric Hg species and wet deposition fluxes using standard techniques should be established. It is important to constrain modeling studies and assess the Hg deposition fluxes in China.
- Better understanding of the atmospheric chemical and physical processes of atmospheric Hg in China is needed. The effects of domestic atmospheric pollutions in China including PM, SO_2, and nitrogen oxides on atmospheric Hg transformations should be evaluated.
- Long-term trend of GEM distribution in ambient air in China is needed. This facilitates understanding in the temporal changes of atmospheric Hg emissions and the response of atmospheric Hg to pollution control measures.

ACPD
15, 11925–11983, 2015

– Outflows and inputs of atmospheric Hg from China into the Chinese marginal seas and the Pacific and its impacts on Hg concentrations in marine water and marine products need to be addressed.

– Using new methods such as Hg isotopes to trace the sources and processes of atmospheric Hg is required.

Acknowledgements. This work was funded by the National "973" Program of China (2013CB430003); the National Science Foundation of China (41473025, 41273145, 41428301). We also acknowledge Lei Zhang, Shuxiao Wang, Tijian Wang, and Laiguo Chen for providing the diurnal and monthly mean atmospheric gaseous mercury concentrations at Miyun, Nanjing, Mt. Dinghu, and Guangzhou.

References

AMAP/UNEP: Technical Background Report for the Global Mercury Assessment 2013, Arctic Monitoring and Assessment Programme, Oslo, Norway/UNEP Chemicals Branch, Geneva, Switzerland., vi + 263 pp., 2013.

Ambrose, J. L., Lyman, S. N., Huang, J. Y., Gustin, M. S., and Jaffe, D. A.: Fast Time Resolution Oxidized Mercury Measurements during the Reno Atmospheric Mercury Intercomparison Experiment (RAMIX), Environ. Sci. Technol., 47, 7285–7294, doi:10.1021/Es303916v, 2013.

An, Z. S.: The history and variability of the East Asian paleomonsoon climate, Quaternary. Sci. Rev., 19, 171–187, doi:10.1016/S0277-3791(99)00060-8, 2000.

Brooks, S., Luke, W., Cohen, M., Kelly, P., Lefer, B., and Rappengluck, B.: Mercury species measured atop the Moody Tower TRAMP site, Houston, Texas, Atmos. Environ., 44, 4045–4055, doi:10.1016/j.atmosenv.2009.02.009, 2010.

Chen, L. G., Liu, M., Xu, Z. C., Fan, R. F., Tao, J., Chen, D. H., Zhang, D. Q., Xie, D. H., and Sun, J. R.: Variation trends and influencing factors of total gaseous mercury in the Pearl River Delta-A highly industrialised region in South China influenced by seasonal monsoons, Atmos. Environ., 77, 757–766, doi:10.1016/j.atmosenv.2013.05.053, 2013.

Choi, E. M., Kim, S. H., Holsen, T. M., and Yi, S. M.: Total gaseous concentrations in mercury in Seoul, Korea: local sources compared to long-range transport from China and Japan, Environ. Pollut., 157, 816–822, doi:10.1016/j.envpol.2008.11.023, 2009.

ACPD
15, 11925–11983, 2015

Choi, H. D., Sharac, T. J., and Holsen, T. M.: Mercury deposition in the Adirondacks: a comparison between precipitation and throughfall, Atmos. Environ., 42, 1818–1827, doi:10.1016/j.atmosenv.2007.11.036, 2008.
Ci, Z. J., Zhang, X. S., Wang, Z. W., and Niu, Z. C.: Atmospheric gaseous elemental mercury (GEM) over a coastal/rural site downwind of East China: temporal variation and long-range transport, Atmos. Environ., 45, 2480–2487, doi:10.1016/j.atmosenv.2011.02.043, 2011a.
Ci, Z. J., Zhang, X. S., Wang, Z. W., Niu, Z. C., Diao, X. Y., and Wang, S. W.: Distribution and air-sea exchange of mercury (Hg) in the Yellow Sea, Atmos. Chem. Phys., 11, 2881–2892, doi:10.5194/acp-11-2881-2011, 2011b.
Cole, A. S., Steffen, A., Pfaffhuber, K. A., Berg, T., Pilote, M., Poissant, L., Tordon, R., and Hung, H.: Ten-year trends of atmospheric mercury in the high Arctic compared to Canadian sub-Arctic and mid-latitude sites, Atmos. Chem. Phys., 13, 1535–1545, doi:10.5194/acp-13-1535-2013, 2013.
Dastoor, A. P. and Larocque, Y.: Global circulation of atmospheric mercury: a modelling study, Atmos. Environ., 38, 147–161, doi:10.1016/j.atmosenv.2003.08.037, 2004.
Demers, J. D., Driscoll, C. T., Fahey, T. J., and Yavitt, J. B.: Mercury cycling in litter and soil in different forest types in the Adirondack region, New York, USA, Ecol. Appl., 17, 1341–1351, doi:10.1890/06-1697.1, 2007.
Dommergue, A., Ferrari, C. P., Planchon, F. A. M., and Boutron, C. F.: Influence of anthropogenic sources on total gaseous mercury variability in grenoble suburban air (France), Sci. Total Environ., 297, 203–213, doi:10.1016/S0048-9697(02)00133-X, 2002.
Dommergue, A., Sprovieri, F., Pirrone, N., Ebinghaus, R., Brooks, S., Courteaud, J., and Ferrari, C. P.: Overview of mercury measurements in the Antarctic troposphere, Atmos. Chem. Phys., 10, 3309–3319, doi:10.5194/acp-10-3309-2010, 2010.
Dou, H. Y., Wang, S. X., Wang, L., Zhang, L., and Hao, J. M.: Characteristics of total gaseous mercury concentrations at a rural site of Yangtze Delta, China, Environ. Sci., 34, 1–7, 2013 (in Chinese).
Driscoll, C. T., Mason, R. P., Chan, H. M., Jacob, D. J., and Pirrone, N.: Mercury as a global pollutant: sources, pathways, and effects, Environ. Sci. Technol., 47, 4967–4983, doi:10.1021/Es305071v, 2013.
Duan, X. Q. and Yang, H.: Pollutions of tmospheric partilucated mercury in urban Lanzhou, Environ. Monitor. Technol., 7, 19–20, 1995 (in Chinese).

ACPD
15, 11925–11983, 2015

Ebinghaus, R., Jennings, S. G., Schroeder, W. H., Berg, T., Donaghy, T., Guentzel, J., Kenny, C., Kock, H. H., Kvietkus, K., Landing, W., Muhleck, T., Munthe, J., Prestbo, E. M., Schneeberger, D., Slemr, F., Sommar, J., Urba, A., Wallschlager, D., and Xiao, Z.: International field intercomparison measurements of atmospheric mercury species at Mace Head, Ireland, Atmos. Environ., 33, 3063–3073, doi:10.1016/S1352-2310(98)00119-8, 1999.

Ebinghaus, R., Kock, H. H., Coggins, A. M., Spain, T. G., Jennings, S. G., and Temme, C.: Long-term measurements of atmospheric mercury at Mace Head, Irish west coast, between 1995 and 2001, Atmos. Environ., 36, 5267–5276, doi:10.1016/S1352-2310(02)00691-X, 2002.

Engle, M. A., Tate, M. T., Krabbenhoft, D. P., Schauer, J. J., Kolker, A., Shanley, J. B., and Bothner, M. H.: Comparison of atmospheric mercury speciation and deposition at nine sites across central and eastern North America, J. Geophys. Res.-Atmos., 115, D18306, doi:10.1029/2010jd014064, 2010.

Faïn, X., Obrist, D., Hallar, A. G., Mccubbin, I., and Rahn, T.: High levels of reactive gaseous mercury observed at a high elevation research laboratory in the Rocky Mountains, Atmos. Chem. Phys., 9, 8049–8060, doi:10.5194/acp-9-8049-2009, 2009.

Fang, F. M., Wang, Q. C., and Li, J. F.: Urban environmental mercury in Changchun, a metropolitan city in Northeastern China: source, cycle, and fate, Sci. Total Environ., 330, 159–170, doi:10.1016/j.scitotenv.2004.04.006, 2004.

Feng, X. B., Shang, L. H., Wang, S. F., Tang, S. L., and Zheng, W.: Temporal variation of total gaseous mercury in the air of Guiyang, China, J. Geophys. Res.-Atmos., 109, D03303, doi:10.1029/2003jd004159, 2004.

Feng, X. B., Wang, S. F., Qiu, G. A., Hou, Y. M., and Tang, S. L.: Total gaseous mercury emissions from soil in Guiyang, Guizhou, China, J. Geophys. Res.-Atmos., 110, D14306, doi:10.1029/2004jd005643, 2005.

Fisher, L. S. and Wolfe, M. H.: Examination of mercury inputs by throughfall and litterfall in the Great Smoky Mountains National Park, Atmos. Environ., 47, 554–559, doi:10.1016/j.atmosenv.2011.10.017, 2012.

Friedli, H. R., Radke, L. F., Prescott, R., Li, P., Woo, J. H., and Carmichael, G. R.: Mercury in the atmosphere around Japan, Korea, and China as observed during the 2001 ACE-Asia field campaign: measurements, distributions, sources, and implications, J. Geophys. Res.-Atmos., 109, D19S25, doi:10.1029/2003jd004244, 2004.

ACPD
15, 11925–11983, 2015

Friedli, H. R., Arellano Jr., A. F., Geng, F., Cai, C., and Pan, L.: Measurements of atmospheric mercury in Shanghai during September 2009, Atmos. Chem. Phys., 11, 3781–3788, doi:10.5194/acp-11-3781-2011, 2011.

Fu, X. W. and Feng, X. B.: Variations of atmospheric total gaseous mercury concentrations for the sampling campaigns of 2001/2002 and 2009/2010 and implications of changes in regional emissions of atmospheric mercury, Bull Miner Petr. Geochem., in press, 2015 (in Chinese).

Fu, X. W., Feng, X. B., and Wang, S. F.: Exchange fluxes of Hg between surfaces and atmosphere in the eastern flank of Mount Gongga, Sichuan province, southwestern China, J. Geophys. Res.-Atmos., 113, D20306, doi:10.1029/2008jd009814, 2008a.

Fu, X. W., Feng, X. B., Zhu, W. Z., Wang, S. F., and Lu, J. L.: Total gaseous mercury concentrations in ambient air in the eastern slope of Mt. Gongga, South-Eastern fringe of the Tibetan plateau, China, Atmos. Environ., 42, 970–979, doi:10.1016/j.atmosenv.2007.10.018, 2008b.

Fu, X. W., Feng, X. B., Zhu, W. Z., Zheng, W., Wang, S. F., and Lu, J. Y.: Total particulate and reactive gaseous mercury in ambient air on the eastern slope of the Mt. Gongga area, China, Appl. Geochem., 23, 408–418, doi:10.1016/j.apgeochem.2007.12.018, 2008c.

Fu, X., Feng, X., Zhu, W., Rothenberg, S., Yao, H., and Zhang, H.: Elevated atmospheric deposition and dynamics of mercury in a remote upland forest of southwestern China, Environ. Pollut., 158, 2324–2333, doi:10.1016/j.envpol.2010.01.032, 2010a.

Fu, X. W., Feng, X., Dong, Z. Q., Yin, R. S., Wang, J. X., Yang, Z. R., and Zhang, H.: Atmospheric gaseous elemental mercury (GEM) concentrations and mercury depositions at a high-altitude mountain peak in south China, Atmos. Chem. Phys., 10, 2425–2437, doi:10.5194/acp-10-2425-2010, 2010b.

Fu, X. W., Feng, X. B., Zhang, G., Xu, W. H., Li, X. D., Yao, H., Liang, P., Li, J., Sommar, J., Yin, R. S., and Liu, N.: Mercury in the marine boundary layer and seawater of the South China Sea: concentrations, sea/air flux, and implication for land outflow, J. Geophys. Res.-Atmos., 115, D06303, doi:10.1029/2009jd012958, 2010c.

Fu, X. W., Feng, X. B., Qiu, G. L., Shang, L. H., and Zhang, H.: Speciated atmospheric mercury and its potential source in Guiyang, China, Atmos. Environ., 45, 4205–4212, doi:10.1016/j.atmosenv.2011.05.012, 2011a.

Fu, X. W., Feng, X. B., and Zhang, H.: Atmospheric total gaseous mercury concentration in Guiyang: measurements intercomparison with Lumex Ra-915AM and Tekran 2537A, Chinese J. Ecol., 30, 939–943, 2011b (in Chinese).

ACPD
15, 11925–11983, 2015

Fu, X. W., Feng, X., Liang, P., Deliger, Zhang, H., Ji, J., and Liu, P.: Temporal trend and sources of speciated atmospheric mercury at Waliguan GAW station, Northwestern China, Atmos. Chem. Phys., 12, 1951–1964, doi:10.5194/acp-12-1951-2012, 2012a.
Fu, X. W., Feng, X., Shang, L. H., Wang, S. F., and Zhang, H.: Two years of measurements of atmospheric total gaseous mercury (TGM) at a remote site in Mt. Changbai area, Northeastern China, Atmos. Chem. Phys., 12, 4215–4226, doi:10.5194/acp-12-4215-2012, 2012b.
Fu, X. W., Feng, X. B., Zhang, H., Yu, B., and Chen, L. G.: Mercury emissions from natural surfaces highly impacted by human activities in Guangzhou province, South China, Atmos. Environ., 54, 185–193, doi:10.1016/j.atmosenv.2012.02.008, 2012c.
Fu, X. W., Feng, X. B., Guo, Y. N., Meng, B., Yin, R. S., and Yao, H.: Distribution and production of reactive mercury and dissolved gaseous mercury in surface waters and water/air mercury flux in reservoirs on Wujiang River, Southwest China, J. Geophys. Res.-Atmos., 118, 3905–3917, doi:10.1002/Jgrd.50384, 2013.
Fu, X. W., Zhang, H., Feng, X. B., and Zhu, W.: Speciated atmospheric mercury in rural Mt. Changbai, Northeast China, 17th Internatial Conference of Heavy Metals in the Environment, Guiyang, China, 219, 22–25 September 2014, 2014.
Fu, X. W., Zhang, H., Lin, C.-J., Feng, X. B., Zhou, L. X., and Fang, S. X.: Correlation slopes of GEM / CO, GEM / CO_2, and GEM / CH_4 and estimated mercury emissions in China, South Asia, the Indochinese Peninsula, and Central Asia derived from observations in northwestern and southwestern China, Atmos. Chem. Phys., 15, 1013–1028, doi:10.5194/acp-15-1013-2015, 2015.
Gardfeldt, K., Sommar, J., Ferrara, R., Ceccarini, C., Lanzillotta, E., Munthe, J., Wangberg, I., Lindqvist, O., Pirrone, N., Sprovieri, F., Pesenti, E., and Stromberg, D.: Evasion of mercury from coastal and open waters of the Atlantic Ocean and the Mediterranean Sea, Atmos. Environ., 37, S73–S84, doi:10.1016/S1352-2310(03)00238-3, 2003.
Graydon, J. A., Louis, V. L. S., Hintelmann, H., Lindberg, S. E., Sandilands, K. A., Rudd, J. W. M., Kelly, C. A., Hall, B. D., and Mowat, L. D.: Long-term wet and dry deposition of total and methyl mercury in the remote boreal ecoregion of Canada, Environ. Sci. Technol., 42, 8345–8351, doi:10.1021/Es801056j, 2008.
Grigal, D. F., Kolka, R. K., Fleck, J. A., and Nater, E. A.: Mercury budget of an upland-peatland watershed, Biogeochemistry, 50, 95–109, doi:10.1023/A:1006322705566, 2000.
Guo, Y. N., Feng, X. B., Li, Z. G., He, T. R., Yan, H. Y., Meng, B., Zhang, J. F., and Qiu, G. L.: Distribution and wet deposition fluxes of total and methyl mercury in Wujiang River Basin,

ACPD
15, 11925–11983, 2015

Guizhou, China, Atmos. Environ., 42, 7096–7103, doi:10.1016/j.atmosenv.2008.06.006, 2008.
Gustin, M. and Jaffe, D.: Reducing the uncertainty in measurement and understanding of mercury in the atmosphere, Environ. Sci. Technol., 44, 2222–2227, doi:10.1021/Es902736k, 2010.
Gustin, M. S., Huang, J. Y., Miller, M. B., Peterson, C., Jaffe, D. A., Ambrose, J., Finley, B. D., Lyman, S. N., Call, K., Talbot, R., Feddersen, D., Mao, H. T., and Lindberg, S. E.: Do we understand what the mercury speciation instruments are actually measuring? Results of RAMIX, Environ. Sci. Technol., 47, 7295–7306, doi:10.1021/Es3039104, 2013.
Hedgecock, I. M. and Pirrone, N.: Chasing quicksilver: modeling the atmospheric lifetime of Hg0(g) in the marine boundary layer at various latitudes, Environ. Sci. Technol., 38, 69–76, doi:10.1021/es034623z, 2003.
Huang, J., Kang, S. C., Zhang, Q. G., Yan, H. Y., Guo, J. M., Jenkins, M. G., Zhang, G. S., and Wang, K.: Wet deposition of mercury at a remote site in the Tibetan Plateau: concentrations, speciation, and fluxes, Atmos. Environ., 62, 540–550, doi:10.1016/j.atmosenv.2012.09.003, 2012.
Huang, J. Y., Miller, M. B., Weiss-Penzias, P., and Gustin, M. S.: Comparison of gaseous oxidized Hg measured by KCl-coated denuders, and nylon and cation exchange membranes, Environ. Sci. Technol., 47, 7307–7316, doi:10.1021/Es4012349, 2013.
Jaffe, D., Prestbo, E., Swartzendruber, P., Weiss-Penzias, P., Kato, S., Takami, A., Hatakeyama, S., and Kajii, Y.: Export of atmospheric mercury from Asia, Atmos. Environ., 39, 3029–3038, doi:10.1016/j.atmosenv.2005.01.030, 2005.
Jaffe, D. A., Lyman, S., Amos, H. M., Gustin, M. S., Huang, J. Y., Selin, N. E., Levin, L., ter Schure, A., Mason, R. P., Talbot, R., Rutter, A., Finley, B., Jaegle, L., Shah, V., McClure, C., Arnbrose, J., Gratz, L., Lindberg, S., Weiss-Penzias, P., Sheu, G. R., Feddersen, D., Horvat, M., Dastoor, A., Hynes, A. J., Mao, H. T., Sonke, J. E., Slemr, F., Fisher, J. A., Ebinghaus, R., Zhang, Y. X., and Edwards, G.: Progress on understanding atmospheric mercury hampered by uncertain measurements, Environ. Sci. Technol., 48, 7204–7206, doi:10.1021/Es5026432, 2014.
Keeler, G., Gratz, L., and Al-Wali, K. I.: Long-term atmospheric mercury wet deposition at Underhill, Vermont, Ecotoxicology, 14, 71–83, 2005.

ACPD
15, 11925–11983, 2015

Kim, K. H., Mishra, V. K., and Hong, S.: The rapid and continuous monitoring of gaseous elemental mercury (GEM) behavior in ambient air, Atmos. Environ., 40, 3281–3293, doi:10.1016/j.atmosenv.2006.01.046, 2006.

Kock, H. H., Bieber, E., Ebinghaus, R., Spain, T. G., and Thees, B.: Comparison of long-term trends and seasonal variations of atmospheric mercury concentrations at the two European coastal monitoring stations Mace Head, Ireland, and Zingst, Germany, Atmos. Environ., 39, 7549–7556, doi:10.1016/j.atmosenv.2005.02.059, 2005.

Lai, S. C., Baker, A. K., Schuck, T. J., Slemr, F., Brenninkmeijer, C. A. M., van Velthoven, P., Oram, D. E., Zahn, A., and Ziereis, H.: Characterization and source regions of 51 high-CO events observed during Civil Aircraft for the Regular Investigation of the Atmosphere Based on an Instrument Container (CARIBIC) flights between south China and the Philippines, 2005–2008, J. Geophys. Res.-Atmos., 116, D20308, doi:10.1029/2011jd016375, 2011.

Lan, X., Talbot, R., Castro, M., Perry, K., and Luke, W.: Seasonal and diurnal variations of atmospheric mercury across the US determined from AMNet monitoring data, Atmos. Chem. Phys., 12, 10569–10582, doi:10.5194/acp-12-10569-2012, 2012.

Landis, M. S. and Keeler, G. J.: Critical evaluation of a modified automatic wet-only precipitation collector for mercury and trace element determinations, Environ. Sci. Technol., 31, 2610–2615, doi:10.1021/Es9700055, 1997.

Landis, M. S., Stevens, R. K., Schaedlich, F., and Prestbo, E. M.: Development and characterization of an annular denuder methodology for the measurement of divalent inorganic reactive gaseous mercury in ambient air, Environ. Sci. Technol., 36, 3000–3009, doi:10.1021/Es015887t, 2002.

Lang, X.: Mercury in atmospheric precipitation and litterfall in Mt.Ailao and Mt.Damei, Master's dissertation, Guizhou University, Guiyang, China, 1–78, 2014 (in Chinese).

Larssen, T., de Wit, H. A., Wiker, M., and Halse, K.: Mercury budget of a small forested boreal catchment in southeast Norway, Sci. Total Environ., 404, 290–296, doi:10.1016/j.scitotenv.2008.03.013, 2008.

Lee, D. S., Dollard, G. J., and Pepler, S.: Gas-phase mercury in the atmosphere of the United Kingdom, Atmos. Environ., 32, 855–864, doi:10.1016/S1352-2310(97)00316-6, 1998.

Lee, Y. H., Bishop, K. H., and Munthe, J.: Do concepts about catchment cycling of methylmercury and mercury in boreal catchments stand the test of time? Six years of atmospheric inputs and runoff export at Svartberget, northern Sweden, Sci. Total Environ., 260, 11–20, doi:10.1016/S0048-9697(00)00538-6, 2000.

ACPD
15, 11925–11983, 2015

Leermakers, M., Baeyens, W., Ebinghaus, R., Kuballa, J., and Kock, H. H.: Determination of atmospheric mercury during the North Sea experiment, Water Air Soil Poll., 97, 257–263, doi:10.1023/A:1018311107587, 1997.
Li, J., Sommar, J., Wangberg, I., Lindqvist, O., and Wei, S. Q.: Short-time variation of mercury speciation in the urban of Goteborg during GOTE-2005, Atmos. Environ., 42, 8382–8388, doi:10.1016/j.atmosenv.2008.08.007, 2008.
Li, P., Feng, X. B., Qiu, G. L., Shang, L. H., Wang, S. F., and Meng, B.: Atmospheric mercury emission from artisanal mercury mining in Guizhou Province, Southwestern China, Atmos. Environ., 43, 2247–2251, doi:10.1016/j.atmosenv.2009.01.050, 2009.
Li, Z.: The concentrations, species and influencing factors of atmospheric mercury in the urban and remote areas: a case study of Chinese cities and Arctic Ocean, Ph.D. thesis, Unicersity of Science and Technology of China, Hefei, China, 1–122, 2012 (in Chinese).
Li, Z., Xia, C. H., Wang, X. M., Xiang, Y. R., and Xie, Z. Q.: Total gaseous mercury in Pearl River Delta region, China during 2008 winter period, Atmos. Environ., 45, 834–838, doi:10.1016/j.atmosenv.2010.11.032, 2011.
Liang, S., Xu, M., Liu, Z., Suh, S., and Zhang, T. Z.: Socioeconomic drivers of mercury emissions in China from 1992 to 2007, Environ. Sci. Technol., 47, 3234–3240, doi:10.1021/Es303728d, 2013.
Lin, C.-J., Pan, L., Streets, D. G., Shetty, S. K., Jang, C., Feng, X., Chu, H.-W., and Ho, T. C.: Estimating mercury emission outflow from East Asia using CMAQ-Hg, Atmos. Chem. Phys., 10, 1853–1864, doi:10.5194/acp-10-1853-2010, 2010.
Lindberg, S., Bullock, R., Ebinghaus, R., Engstrom, D., Feng, X. B., Fitzgerald, W., Pirrone, N., Prestbo, E., and Seigneur, C.: A synthesis of progress and uncertainties in attributing the sources of mercury in deposition, Ambio, 36, 19–32, 2007.
Lindberg, S. E., Brooks, S., Lin, C. J., Scott, K. J., Landis, M. S., Stevens, R. K., Goodsite, M., and Richter, A.: Dynamic oxidation of gaseous mercury in the Arctic troposphere at polar sunrise, Environ. Sci. Technol., 36, 1245–1256, doi:10.1021/Es0111941, 2002.
Liu, B., Keeler, G. J., Dvonch, J. T., Barres, J. A., Lynam, M. M., Marsik, F. J., and Morgan, J. T.: Urban-rural differences in atmospheric mercury speciation, Atmos. Environ., 44, 2013–2023, doi:10.1016/j.atmosenv.2010.02.012, 2010.
Liu, N., Qiu, G. L., Feng, X. B., Landis, M., Fu, X. W., and Shang, L. H.: Distribution characteristics of mercury in precipitation of Guiyang, China, Chinese J. Ecol., 30, 933–938, 2011 (in Chinese).

ACPD
15, 11925–11983, 2015

Liu, S. L., Nadim, F., Perkins, C., Carley, R. J., Hoag, G. E., Lin, Y. H., and Chen, L. T.: Atmospheric mercury monitoring survey in Beijing, China, Chemosphere, 48, 97–107, doi:10.1016/S0045-6535(02)00026-7, 2002.
Lyman, S. N. and Jaffe, D. A.: Formation and fate of oxidized mercury in the upper troposphere and lower stratosphere, Nat. Geosci., 5, 114–117, doi:10.1038/Ngeo1353, 2012.
Lynam, M. M. and Keeler, G. J.: Comparison of methods for particulate phase mercury analysis: sampling and analysis, Anal. Bioanal. Chem., 374, 1009–1014, doi:10.1007/s00216-002-1584-4, 2002.
Lyman, S. N., Jaffe, D. A., and Gustin, M. S.: Release of mercury halides from KCl denuders in the presence of ozone, Atmos. Chem. Phys., 10, 8197–8204, doi:10.5194/acp-10-8197-2010, 2010.
Mason, R. P. and Sheu, G. R.: Role of the ocean in the global mercury cycle, Global Biogeochem. Cy., 16, 1093, doi:10.1029/2001gb001440, 2002.
Mason, R. P., Lawson, N. M., and Sheu, G. R.: Annual and seasonal trends in mercury deposition in Maryland, Atmos. Environ., 34, 1691–1701, doi:10.1016/S1352-2310(99)00428-8, 2000.
McClure, C. D., Jaffe, D. A., and Edgerton, E. S.: Evaluation of the KCl denuder method for gaseous oxidized mercury using $HgBr_2$ at an in-service AMNet site, Environ. Sci. Technol., 48, 11437–11444, doi:10.1021/Es502545k, 2014.
Moore, C. W., Obrist, D., and Luria, M.: Atmospheric mercury depletion events at the Dead Sea: spatial and temporal aspects, Atmos. Environ., 69, 231–239, doi:10.1016/j.atmosenv.2012.12.020, 2013.
Müller, D., Wip, D., Warneke, T., Holmes, C. D., Dastoor, A., and Notholt, J.: Sources of atmospheric mercury in the tropics: continuous observations at a coastal site in Suriname, Atmos. Chem. Phys., 12, 7391–7397, doi:10.5194/acp-12-7391-2012, 2012.
Muntean, M., Janssens-Maenhout, G., Song, S. J., Selin, N. E., Olivier, J. G. J., Guizzardi, D., Maas, R., and Dentener, F.: Trend analysis from 1970 to 2008 and model evaluation of EDGARv4 global gridded anthropogenic mercury emissions, Sci. Total Environ., 494, 337–350, doi:10.1016/j.scitotenv.2014.06.014, 2014.
Munthe, J., Hultberg, H., and Iverfeldt, A.: Mechanisms of deposition of methylmercury and mercury to coniferous forests, Water Air Soil Poll., 80, 363–371, doi:10.1007/Bf01189686, 1995.

ACPD
15, 11925–11983, 2015

Munthe, J., Wangberg, I., Iverfeldt, A., Lindqvist, O., Stromberg, D., Sommar, J., Gardfeldt, K., Petersen, G., Ebinghaus, R., Prestbo, E., Larjava, K., and Siemens, V.: Distribution of atmospheric mercury species in Northern Europe: final results from the MOE project, Atmos. Environ., 37, S9–S20, doi:10.1016/S1352-2310(03)00235-8, 2003.

Murphy, D. M., Thomson, D. S., and Mahoney, T. M. J.: In situ measurements of organics, meteoritic material, mercury, and other elements in aerosols at 5 to 19 kilometers, Science, 282, 1664–1669, doi:10.1126/science.282.5394.1664, 1998.

National Bureau of Statistics of China, P. R. C.: China Energy Statistical Yearbook (2005–2011), China Statistics Press, Beijing, China, 2012.

Nguyen, D. L., Kim, J. Y., Shim, S. G., and Zhang, X. S.: Ground and shipboard measurements of atmospheric gaseous elemental mercury over the Yellow Sea region during 2007–2008, Atmos. Environ., 45, 253–260, doi:10.1016/j.atmosenv.2010.07.021, 2011.

Nguyen, H. T., Kim, M. Y., and Kim, K. H.: The influence of long-range transport on atmospheric mercury on Jeju Island, Korea, Sci. Total Environ., 408, 1295–1307, doi:10.1016/j.scitotenv.2009.10.029, 2010.

Pacyna, E. G., Pacyna, J. M., Sundseth, K., Munthe, J., Kindbom, K., Wilson, S., Steenhuisen, F., and Maxson, P.: Global emission of mercury to the atmosphere from anthropogenic sources in 2005 and projections to 2020, Atmos. Environ., 44, 2487–2499, doi:10.1016/j.atmosenv.2009.06.009, 2010.

Pacyna, J. M., Pacyna, E. G., Steenhuisen, F., and Wilson, S.: Mapping 1995 global anthropogenic emissions of mercury, Atmos. Environ., 37, S109–S117, doi:10.1016/S1352-2310(03)00239-5, 2003.

Pan, L., Woo, J. H., Carmichael, G. R., Tang, Y. H., Friedli, H. R., and Radke, L. F.: Regional distribution and emissions of mercury in east Asia: a modeling analysis of Asian Pacific Regional Aerosol Characterization Experiment (ACE-Asia) observations, J. Geophys. Res.-Atmos., 111, D07109, doi:10.1029/2005jd006381, 2006.

Pan, L., Chai, T. F., Carmichael, G. R., Tang, Y. H., Streets, D., Woo, J. H., Friedli, H. R., and Radke, L. F.: Top-down estimate of mercury emissions in China using four-dimensional variational data assimilation, Atmos. Environ., 41, 2804–2819, doi:10.1016/j.atmosenv.2006.11.048, 2007.

Peterson, C., Gustin, M., and Lyman, S.: Atmospheric mercury concentrations and speciation measured from 2004 to 2007 in Reno, Nevada, USA, Atmos. Environ., 43, 4646–4654, doi:10.1016/j.atmosenv.2009.04.053, 2009.

ACPD
15, 11925–11983, 2015

Pirrone, N., Keeler, G. J., and Nriagu, J. O.: Regional differences in worldwide emissions of mercury to the atmosphere, Atmos. Environ., 30, 2981–2987, doi:10.1016/1352-2310(95)00498-X, 1996.
Pirrone, N., Cinnirella, S., Feng, X., Finkelman, R. B., Friedli, H. R., Leaner, J., Mason, R., Mukherjee, A. B., Stracher, G. B., Streets, D. G., and Telmer, K.: Global mercury emissions to the atmosphere from anthropogenic and natural sources, Atmos. Chem. Phys., 10, 5951–5964, doi:10.5194/acp-10-5951-2010, 2010.
Poissant, L., Pilote, M., Beauvais, C., Constant, P., and Zhang, H. H.: A year of continuous measurements of three atmospheric mercury species (GEM, RGM and Hg-p) in southern Quebec, Canada, Atmos. Environ., 39, 1275–1287, doi:10.1016/j.atmosenv.2004.11.007, 2005.
Prestbo, E. and Gay, D. A.: Wet deposition of mercury in the US and Canada, 1996–2005: Results and analysis of the NADP mercury deposition network (MDN), Atmos. Environ., 43, 4223–4233, 2009.
Rea, A. W., Lindberg, S. E., and Keeler, G. J.: Dry deposition and foliar leaching of mercury and selected trace elements in deciduous forest throughfall, Atmos. Environ., 35, 3453–3462, doi:10.1016/S1352-2310(01)00133-9, 2001.
Ren, W., Duan, L., Zhu, Z. W., Du, W., An, Z. Y., Xu, L. J., Zhang, C., Zhuo, Y. Q., and Chen, C. H.: Mercury Transformation and Distribution Across a Polyvinyl Chloride (PVC) Production Line in China, Environ. Sci. Technol., 48, 2321–2327, doi:10.1021/Es404147c, 2014.
Schroeder, W. H. and Munthe, J.: Atmospheric mercury – an overview, Atmos. Environ., 32, 809–822, doi:10.1016/S1352-2310(97)00293-8, 1998.
Schroeder, W. H., Anlauf, K. G., Barrie, L. A., Lu, J. Y., Steffen, A., Schneeberger, D. R., and Berg, T.: Arctic springtime depletion of mercury, Nature, 394, 331–332, doi:10.1038/28530, 1998.
Schwesig, D. and Matzner, E.: Pools and fluxes of mercury and methylmercury in two forested catchments in Germany, Sci. Total Environ., 260, 213–223, doi:10.1016/S0048-9697(00)00565-9, 2000.
Selin, N. E., Jacob, D. J., Park, R. J., Yantosca, R. M., Strode, S., Jaegle, L., and Jaffe, D.: Chemical cycling and deposition of atmospheric mercury: global constraints from observations, J. Geophys. Res.-Atmos., 112, D02308, doi:10.1029/2006jd007450, 2007.
Sexauer Gustin, M., Amos, H. M., Huang, J., Miller, M. B., and Heidecorn, K.: Successes and challenges of measuring and modeling atmospheric mercury at the part per quadrillion level:

ACPD
15, 11925–11983, 2015

a critical review, Atmos. Chem. Phys. Discuss., 15, 3777–3821, doi:10.5194/acpd-15-3777-2015, 2015.
Shetty, S. K., Lin, C. J., Streets, D. G., and Jang, C.: Model estimate of mercury emission from natural sources in East Asia, Atmos. Environ., 42, 8674–8685, doi:10.1016/j.atmosenv.2008.08.026, 2008.
Sheu, G. R., Lin, N. H., Wang, J. L., Lee, C. T., Yang, C. F. O., and Wang, S. H.: Temporal distribution and potential sources of atmospheric mercury measured at a high-elevation background station in Taiwan, Atmos. Environ., 44, 2393–2400, doi:10.1016/j.atmosenv.2010.04.009, 2010.
Sheu, G. R., Lin, N. H., Lee, C. T., Wang, J. L., Chuang, M. T., Wang, S. H., Chi, K. H., and Ou-Yang, C. F.: Distribution of atmospheric mercury in northern Southeast Asia and South China Sea during Dongsha Experiment, Atmos. Environ., 78, 174–183, doi:10.1016/j.atmosenv.2012.07.002, 2013.
Slemr, F. and Scheel, H. E.: Trends in atmospheric mercury concentrations at the summit of the Wank mountain, southern Germany, Atmos. Environ., 32, 845–853, doi:10.1016/S1352-2310(97)00131-3, 1998.
Slemr, F., Brunke, E. G., Ebinghaus, R., Temme, C., Munthe, J., Wangberg, I., Schroeder, W., Steffen, A., and Berg, T.: Worldwide trend of atmospheric mercury since 1977, Geophys. Res. Lett., 30, 1516, doi:10.1029/2003gl016954, 2003.
Slemr, F., Ebinghaus, R., Brenninkmeijer, C. A. M., Hermann, M., Kock, H. H., Martinsson, B. G., Schuck, T., Sprung, D., van Velthoven, P., Zahn, A., and Ziereis, H.: Gaseous mercury distribution in the upper troposphere and lower stratosphere observed onboard the CARIBIC passenger aircraft, Atmos. Chem. Phys., 9, 1957–1969, doi:10.5194/acp-9-1957-2009, 2009.
Slemr, F., Brunke, E.-G., Ebinghaus, R., and Kuss, J.: Worldwide trend of atmospheric mercury since 1995, Atmos. Chem. Phys., 11, 4779–4787, doi:10.5194/acp-11-4779-2011, 2011.
Slemr, F., Weigelt, A., Ebinghaus, R., Brenninkmeijer, C., Baker, A., Schuck, T., Rauthe-Schoch, A., Riede, H., Leedham, E., Hermann, M., van Velthoven, P., Oram, D., O'Sullivan, D., Dyroff, C., Zahn, A., and Ziereis, H.: Mercury plumes in the global upper troposphere observed during flights with the CARIBIC observatory from May 2005 until June 2013, Atmosphere-Basel, 5, 342–369, doi:10.3390/Atmos5020342, 2014.
Slemr, F., Angot, H., Dommergue, A., Magand, O., Barret, M., Weigelt, A., Ebinghaus, R., Brunke, E.-G., Pfaffhuber, K. A., Edwards, G., Howard, D., Powell, J., Keywood, M., and

ACPD
15, 11925–11983, 2015

Wang, F.: Comparison of mercury concentrations measured at several sites in the Southern Hemisphere, Atmos. Chem. Phys., 15, 3125–3133, doi:10.5194/acp-15-3125-2015, 2015.
Song, X. J., Cheng, I., and Lu, J.: Annual atmospheric mercury species in Downtown Toronto, Canada, J. Environ. Monitor., 11, 660–669, doi:10.1039/B815435j, 2009.
Sprovieri, F. and Pirrone, N.: Spatial and temporal distribution of atmospheric mercury species over the Adriatic Sea, Environ. Fluid Mech., 8, 117–128, doi:10.1007/s10652-007-9045-4, 2008.
St Louis, V. L., Rudd, J. W. M., Kelly, C. A., Hall, B. D., Rolfhus, K. R., Scott, K. J., Lindberg, S. E., and Dong, W.: Importance of the forest canopy to fluxes of methyl mercury and total mercury to boreal ecosystems, Environ. Sci. Technol., 35, 3089–3098, doi:10.1021/Es001924p, 2001.
Streets, D. G., Yarber, K. F., Woo, J. H., and Carmichael, G. R.: Biomass burning in Asia: annual and seasonal estimates and atmospheric emissions, Global Biogeochem. Cy., 17, 1099, doi:10.1029/2003gb002040, 2003.
Streets, D. G., Hao, J. M., Wu, Y., Jiang, J. K., Chan, M., Tian, H. Z., and Feng, X. B.: Anthropogenic mercury emissions in China, Atmos. Environ., 39, 7789–7806, doi:10.1016/j.atmosenv.2005.08.029, 2005.
Strode, S. A., Jaegle, L., Jaffe, D. A., Swartzendruber, P. C., Selin, N. E., Holmes, C., and Yantosca, R. M.: Trans-Pacific transport of mercury, J. Geophys. Res.-Atmos., 113, D15305, doi:10.1029/2007jd009428, 2008.
Su, J., Cheng, J. P., Ye, X. F., Yuan, T., Wang, W. H., and Mi, L. J.: Preliminary study on mercury distribution in multimedia environment in Lanzhou, J. Agro-Environ. Sci., 26, 381–385, 2007 (in Chinese).
Swartzendruber, P. C., Jaffe, D. A., Prestbo, E. M., Weiss-Penzias, P., Selin, N. E., Park, R., Jacob, D. J., Strode, S., and Jaegle, L.: Observations of reactive gaseous mercury in the free troposphere at the Mount Bachelor Observatory, J. Geophys. Res.-Atmos., 111, D24302, doi:10.1029/2006jd007415, 2006.
Talbot, R., Mao, H., Scheuer, E., Dibb, J., and Avery, M.: Total depletion of Hg degrees in the upper troposphere-lower stratosphere, Geophys. Res. Lett., 34, L23804, doi:10.1029/2007gl031366, 2007.
Temme, C., Slemr, F., Ebinghaus, R., and Einax, J. W.: Distribution of mercury over the Atlantic Ocean in 1996 and 1999–2001, Atmos. Environ., 37, 1889–1897, doi:10.1016/S1352-2310(03)00069-4, 2003.

ACPD
15, 11925–11983, 2015

Timonen, H., Ambrose, J. L., and Jaffe, D. A.: Oxidation of elemental Hg in anthropogenic and marine airmasses, Atmos. Chem. Phys., 13, 2827–2836, doi:10.5194/acp-13-2827-2013, 2013.

USEPA: Method 1630: Methyl Mercury in Water by Distillation, Aqueous Ethylation, Purge and Trap, and Cold Vapor Atomic Fluorescence Spectrometry, Washington, D.C., USA, 1–55, 1998.

USEPA: Method 1631, Revision E: Mercury in Water by Oxidation, Purge and Trap, and Cold Vapor Atomic Fluorescence Spectrometry, United States Environmental Protection Agency, Washington, D.C., USA, 10–46, 2002.

USGS: U. S. Geological survey Minerals Yearbook-2013 (mercury), US Geological Survery Publications, Reston, VA, USA, 2014.

van Donkelaar, A., Martin, R. V., Brauer, M., Kahn, R., Levy, R., Verduzco, C., and Villeneuve, P. J.: Global estimates of ambient fine particulate matter concentrations from satellite-based aerosol optical depth: development and application, Environ. Health Persp., 118, 847–855, doi:10.1289/Ehp.0901623, 2010.

Wan, Q., Feng, X. B., Lu, J., Zheng, W., Song, X. J., Li, P., Han, S. J., and Xu, H.: Atmospheric mercury in Changbai Mountain area, northeastern China II. The distribution of reactive gaseous mercury and particulate mercury and mercury deposition fluxes, Environ. Res., 109, 721–727, doi:10.1016/j.envres.2009.05.006, 2009a.

Wan, Q., Feng, X. B., Lu, J. L., Zheng, W., Song, X. J., Han, S. J., and Xu, H.: Atmospheric mercury in Changbai Mountain area, northeastern China I. The seasonal distribution pattern of total gaseous mercury and its potential sources, Environ. Res., 109, 201–206, doi:10.1016/j.envres.2008.12.001, 2009b.

Wang, D. Y., He, L., Shi, X. J., Wei, S. Q., and Feng, X. B.: Release flux of mercury from different environmental surfaces in Chongqing, China, Chemosphere, 64, 1845–1854, doi:10.1016/j.chemosphere.2006.01.054, 2006a.

Wang, L., Wang, S. X., Zhang, L., Wang, Y. X., Zhang, Y. X., Nielsen, C., McElroy, M. B., and Hao, J. M.: Source apportionment of atmospheric mercury pollution in China using the GEOS-Chem model, Environ. Pollut., 190, 166–175, doi:10.1016/j.envpol.2014.03.011, 2014a.

Wang, S. F., Feng, X. B., Qiu, G. L., and Fu, X. W.: Comparison of Air/soil mercury exchange between warm and cold season in Hongfeng reservoir region, Environ. Sci., 25, 123–127, 2004 (in Chinese).

ACPD
15, 11925–11983, 2015

Wang, S. X., Zhang, L., Wang, L., Wu, Q. R., Wang, F. Y., and Hao, J. M.: A review of atmospheric mercury emissions, pollution and control in China, Front. Environ. Sci. Eng., 8, 631–649, doi:10.1007/s11783-014-0673-x, 2014b.

Wang, Z. W., Zhang, X. S., Chen, Z. S., and Zhang, Y.: Mercury concentrations in size-fractionated airborne particles at urban and suburban sites in Beijing, China, Atmos. Environ., 40, 2194–2201, doi:10.1016/j.atmosenv.2005.12.003, 2006b.

Wang, Z. W., Chen, Z. S., Duan, N., and Zhang, X. S.: Gaseous elemental mercury concentration in atmosphere at urban and remote sites in China, J. Environ. Sci.-China, 19, 176–180, doi:10.1016/S1001-0742(07)60028-X, 2007.

Wang, Z. W., Zhang, X. S., Xiao, J. S., Zhijia, C., and Yu, P. Z.: Mercury fluxes and pools in three subtropical forested catchments, southwest China, Environ. Pollut., 157, 801–808, doi:10.1016/j.envpol.2008.11.018, 2009.

Wang, Y. M., Wang, D. Y., Meng, B., Peng, Y. L., Zhao, L., and Zhu, J. S.: Spatial and temporal distributions of total and methyl mercury in precipitation in core urban areas, Chongqing, China, Atmos. Chem. Phys., 12, 9417–9426, doi:10.5194/acp-12-9417-2012, 2012.

Wang, Y. M., Peng, Y. L., Wang, D. Y., and Zhang, C.: Wet deposition fluxes of total mercury and methylmercury in core urban areas, Chongqing, China, Atmos. Environ., 92, 87–96, doi:10.1016/j.atmosenv.2014.03.059, 2014c.

Wangberg, I., Schmolke, S., Schager, P., Munthe, J., Ebinghaus, R., and Iverfeldt, A.: Estimates of air–sea exchange of mercury in the Baltic Sea, Atmos. Environ., 35, 5477–5484, doi:10.1016/S1352-2310(01)00246-1, 2001.

Wangberg, I., Munthe, J., Berg, T., Ebinghaus, R., Kock, H. H., Temme, C., Bieber, E., Spain, T. G., and Stolk, A.: Trends in air concentration and deposition of mercury in the coastal environment of the North Sea Area, Atmos. Environ., 41, 2612–2619, doi:10.1016/j.atmosenv.2006.11.024, 2007.

Weiss-Penzias, P., Jaffe, D. A., Swartzendruber, P., Dennison, J. B., Chand, D., Hafner, W., and Prestbo, E.: Observations of Asian air pollution in the free troposphere at Mount Bachelor Observatory during the spring of 2004, J. Geophys. Res.-Atmos., 111, D10304, doi:10.1029/2005jd006522, 2006.

Weiss-Penzias, P., Jaffe, D., Swartzendruber, P., Hafner, W., Chand, D., and Prestbo, E.: Quantifying Asian and biomass burning sources of mercury using the Hg/CO ratio in pollution plumes observed at the Mount Bachelor Observatory, Atmos. Environ., 41, 4366–4379, doi:10.1016/j.atmosenv.2007.01.058, 2007.

ACPD
15, 11925–11983, 2015

Wu, P. P.: Studies on temporal and spatial distributions of atmospheric mercury in Taiwan Strait inshore areas, M.S. thesis, Xiamen Universitry, Xiamen, China, 102 p., 2014 (in Chinese).
Wu, Y., Wang, S. X., Streets, D. G., Hao, J. M., Chan, M., and Jiang, J. K.: Trends in anthropogenic mercury emissions in China from 1995 to 2003, Environ. Sci. Technol., 40, 5312–5318, doi:10.1021/Es060406x, 2006.
Xia, C. H., Xie, Z. Q., and Sun, L. G.: Atmospheric mercury in the marine boundary layer along a cruise path from Shanghai, China to Prydz Bay, Antarctica, Atmos. Environ., 44, 1815–1821, doi:10.1016/j.atmosenv.2009.12.039, 2010.
Xiang, J. Q. and Liu, G. J.: Distribution and sources of atmospheric mercury in urban areas of Wuhan, Resour. Environ. Eng., 22, 27–30, 2008 (in Chinese).
Xiu, G. L., Cai, J., Zhang, W. Y., Zhang, D. N., Bueler, A., Lee, S. C., Shen, Y., Xu, L. H., Huang, X. J., and Zhang, P.: Speciated mercury in size-fractionated particles in Shanghai ambient air, Atmos. Environ., 43, 3145–3154, doi:10.1016/j.atmosenv.2008.07.044, 2009.
Xiu, G. L. L., Jin, Q. X., Zhang, D. N., Shi, S. Y., Huang, X. J., Zhang, W. Y., Bao, L., Gao, P. T., and Chen, B.: Characterization of size-fractionated particulate mercury in Shanghai ambient air, Atmos. Environ., 39, 419–427, doi:10.1016/j.atmosenv.2004.09.046, 2005.
Xu, L. L., Chen, J. S., Niu, Z. C., Yin, L. Q., and Chen, Y. T.: Characterization of mercury in atmospheric particulate matter in the southeast coastal cities of China, Atmos. Pollut. Res., 4, 454–461, doi:10.5094/Apr.2013.052, 2013.
Xu, L. L., Chen, J. S., Yang, L. M., Niu, Z. C., Tong, L., Yin, L. Q., and Chen, Y. T.: Characteristics and sources of atmospheric mercury speciation in a coastal city, Xiamen, China, Chemosphere, 119, 530–539, 2015.
Yang, Y. K., Chen, H., and Wang, D. Y.: Spatial and temporal distribution of gaseous elemental mercury in Chongqing, China, Environ. Monit. Assess., 156, 479–489, doi:10.1007/s10661-008-0499-8, 2009.
Yu, B., Wang, X., Lin, C. J., Fu, X. W., Zhang, H., Shang, L. H., and Feng, X. B.: Atmospheric mercury; Speciation; Pollutant transport; Potential Source Contribution Function; Monsoon; Air quality index, Atmos. Environ., in review, 2015.
Zhang, H., Fu, X. W., Lin, C.-J., Wang, X., and Feng, X. B.: Observation and analysis of speciated atmospheric mercury in Shangri-La, Tibetan Plateau, China, Atmos. Chem. Phys., 15, 653–665, doi:10.5194/acp-15-653-2015, 2015a.

ACPD
15, 11925–11983, 2015

Zhang, H., Fu, X. W., Lin, C. J., Wang, X., Feng, X. B., Yu, B., Zhou, J., and Zhang, Y. P.: Impacts of Indian summer monsoon on distribution of atmospheric mercury at a high-altitude background station, southwestern China, in preparation, 2015b.
Zhang, L., Blanchard, P., Gay, D. A., Prestbo, E. M., Risch, M. R., Johnson, D., Narayan, J., Zsolway, R., Holsen, T. M., Miller, E. K., Castro, M. S., Graydon, J. A., Louis, V. L. St., and Dalziel, J.: Estimation of speciated and total mercury dry deposition at monitoring locations in eastern and central North America, Atmos. Chem. Phys., 12, 4327–4340, doi:10.5194/acp-12-4327-2012, 2012.
Zhang, L., Wang, S. X., Wang, L., and Hao, J. M.: Atmospheric mercury concentration and chemical speciation at a rural site in Beijing, China: implications of mercury emission sources, Atmos. Chem. Phys., 13, 10505–10516, doi:10.5194/acp-13-10505-2013, 2013.
Zhang, L. M., Gong, S. L., Padro, J., and Barrie, L.: A size-segregated particle dry deposition scheme for an atmospheric aerosol module, Atmos. Environ., 35, 549–560, doi:10.1016/S1352-2310(00)00326-5, 2001.
Zhang, L. M., Wright, L. P., and Blanchard, P.: A review of current knowledge concerning dry deposition of atmospheric mercury, Atmos. Environ., 43, 5853–5864, doi:10.1016/j.atmosenv.2009.08.019, 2009.
Zhang, Y. Q., Liu, R. H., Cui, Y. Q., Zhou, J. P., and Wang, Y.: The characteristic analysis of atmospheric mercury during haze days in Qingdao, Chinese Environ. Sci., 34, 1905–1911, 2014 (in Chinese).
Zhao, Y., Nielsen, C. P., McElroy, M. B., Zhang, L., and Zhang, J.: CO emissions in China: uncertainties and implications of improved energy efficiency and emission control, Atmos. Environ., 49, 103–113, doi:10.1016/j.atmosenv.2011.12.015, 2012.
Zheng, J. Y., Ou, J. M., Mo, Z. W., and Yin, S. S.: Mercury emission inventory and its spatial characteristics in the Pearl River Delta region, China, Sci. Total Environ., 412, 214–222, doi:10.1016/j.scitotenv.2011.10.024, 2011.
Zhou, J., Feng, X. B., Liu, H. Y., Zhang, H., Fu, X. W., Bao, Z. D., Wang, X., and Zhang, Y. P.: Examination of total mercury inputs by precipitation and litterfall in a remote upland forest of Southwestern China, Atmos. Environ., 81, 364–372, doi:10.1016/j.atmosenv.2013.09.010, 2013.
Zhu, J., Wang, T., Talbot, R., Mao, H., Hall, C. B., Yang, X., Fu, C., Zhuang, B., Li, S., Han, Y., and Huang, X.: Characteristics of atmospheric Total Gaseous Mercury (TGM) observed in

ACPD
15, 11925–11983, 2015

urban Nanjing, China, Atmos. Chem. Phys., 12, 12103–12118, doi:10.5194/acp-12-12103-2012, 2012.
Zhu, J., Wang, T., Talbot, R., Mao, H., Yang, X., Fu, C., Sun, J., Zhuang, B., Li, S., Han, Y., and Xie, M.: Characteristics of atmospheric mercury deposition and size-fractionated particulate mercury in urban Nanjing, China, Atmos. Chem. Phys., 14, 2233–2244, doi:10.5194/acp-14-2233-2014, 2014.

ACPD
15, 11925–11983, 2015

Table 1. Atmospheric Hg concentrations at ground-based stations in China and other regions worldwide (PBM/TPM: * indicates TPM (total particulate bounded mercury) and the rest indicates PBM (fine (< 2.5 μm) particulate bounded mercury)).

Site	Location			Type	Study period	GEM	PBM/TPM	GOM	Reference
	Lon	Lat	Altitude (m a.s.l.)			(ng m^{-3})	(pg m^{-3})	(pg m^{-3})	
Mt. Changbai	128.112° E	42.402° N	740	Remote	Oct 2008–Oct 2010	1.60 ± 0.51			Fu et al. (2012b)
					Jul 2013–Jul 2014	1.73 ± 0.48	18.9 ± 15.6	5.7 ± 6.8	Fu et al. (2014a)
Mt. Waliguan	100.898° E	36.287° N	3816	Remote	Sep 2007–Sep 2008	1.98 ± 0.98	19.4 ± 18.0	7.4 ± 4.8	Fu et al. (2012a)
Mt. Ailao	101.017° E	24.533° N	2450	Remote	May 2011–May 2012	2.09 ± 0.63	31.3 ± 28.0	2.2 ± 2.3	Zhang et al. (2015b)
Chengshantou	122.68° E	37.38° N	30	Remote	Jul and Oct 2007, Jan and Apr 2009	2.31 ± 0.74			Ci et al. (2011a)
Chongming Island	121.908° E	31.522° N	11	Remote	Sep–Dec 2009	2.50 ± 1.50			Dou et al. (2013)
Shangri-La	99.733° E	28.017° N	3580	Remote	Nov 2009–Oct 2010	2.55 ± 2.73	37.8 ± 31.0	7.9 ± 7.9	Zhang et al. (2015a)
Mt. Leigong	108.2° E	26.39° N	2178	Remote	May 2008–May 2009	2.80 ± 1.51			Fu et al. (2010b)
Wanqingsha	113.55° E	22.7° N	3	Remote	Nov–Dec 2009	2.94			Li et al. (2011)
Miyun	116.775° E	40.481° N	220	Remote	Dec 2008–Nov 2009	3.22 ± 1.94	98.2 ± 113	10.1 ± 18.8	Zhang et al. (2013)
Mt. Damei	121.565° E	29.632° N	550	Remote	Apr 2011–Apr 2013	3.31 ± 1.44	154 ± 104	6.3 ± 3.9	Yu et al. (2015)
Mt. Gongga	102.117° E	29.649° N	1640	Remote	May 2005–Jul 2007	3.98 ± 1.62	30.7 ± 32.0*	6.2 ± 3.9	Fu et al. (2008b, c)
Mt. Dinghu	112.549° E	23.164° N	700	Remote	Sep 2009–Apr 2010	5.07 ± 2.89			Chen et al. (2013)
Mt. Jiuxian	118.11° E	25.71° N	1700	Remote	Nov 2010, Jan, Apr and Aug 2011		24.0 ± 14.6		Xu et al. (2013)
Shanghai	121.54° E	31.23° N	19	Urban	Jul–Sep 2009	2.70 ± 1.70			Friedli et al. (2011)
					Jul 2004–Apr 2006		560 ± 220*		Xiu et al. (2009)
Qingdao	120.5° E	36.16° N	40	Urban	Jan 2013	2.80 ± 0.90	245 ± 174*		Zhang et al. (2014)
Xiamen	118.05° E	24.60° N	7	Urban	Mar 2012–Feb 2013	3.50 ± 1.61	174 ± 280	61 ± 69	Xu et al. (2015)
Ningbo	121.544° E	29.867° N	10	Urban	Oct 2007–Jan 2008	3.79 ± 1.29			Nguyen et al. (2011)
Guangzhou	113.355° E	23.124° N	60	Urban	Nov 2010–Oct 2011	4.60 ± 1.60			Chen et al. (2013)
Jiaxing	120.7° E	30.833° N	10	Urban	Sep 2005	5.40 ± 4.10			Wang et al. (2007)
Chongqing	106.5° E	29.6° N	350	Urban	Aug 2006–Sep 2007	6.74 ± 0.37			Yang et al. (2009)
Nanjing	118.78° E	32.05° N	100	Urban	Jan–Dec 2011	7.90 ± 7.00			Zhu et al. (2012)
					Jun 2011–Feb 2012		1100 ± 570*		Zhu et al. (2014)
Guiyang	106.72° E	26.57° N	1040	Urban	Nov 2011–Nov 2002	8.40 ± 4.87			Feng et al. (2004)
					Dec 2009–Nov 2010	10.2 ± 7.06			Fu and Feng (2015)
					Aug–Dec 2009	9.72 ± 10.2	368 ± 276	35.7 ± 43.9	Fu et al. (2011a)
Beijing	116.392° E	38.898° N	48	Urban	Feb and Sep 1998	10.4 ± 3.25			Liu et al. (2002)
					Jan–Dec 2003		1180 ± 820*		Wang et al. (2006b)
Wuhan	114.3° E	30.6° N	20	Urban	–/2002	14.8			Xiang and Liu (2008)
Changchun	125.319° E	43.824° N	270	Urban	–/2001	18.4	276*		Fang et al. (2004)
Lanzhou	103.79° E	36.067° N	1540	Urban	–/2004	28.6			Su et al. (2007)
					Apr, Jul, Oct and Dec 1994		955*		Duan and Yang (1995)
Southeast coastal cities				Urban	Nov 2010, Jan, Apr and Aug 2011		141 ± 128		Xu et al. (2013)
Suriname, South America	56.983° W	5.933° N		Remote	Mar–Jul 2007	1.40			Muller et al. (2012)
Cape point, South Africa	18.483° E	34.35° S	230	Remote	Jan–Dec 2009	0.87			Slemr et al. (2011)
Cape Grim, Australia	144.683° E	40.683° S		Remote	2011–2013	0.85–0.96			Slemr et al. (2014a)
North America				Urban		1.60–4.50	2.5–25.4	6.9–37.2	Peterson et al. (2009); Song et al. (2009); Engle et al. (2010); Liu et al. (2010); Brooks et al. (2010); Lan et al. (2012)
				Remote		1.32–1.66	1.6–13.7	0.5–5.6	Lan et al. (2012); Cole et al. (2013)
Europe				Urban		1.9–3.4	12.5	2.5	Dommergue et al. (2002); Li et al. (2008)
				Remote		1.40–1.93	3.0–32.2	9.1–26.5	Slemr and Scheel (1998); Lee et al. (1998); Munthe et al. (2003); Kock et al. (2005)
Antarctic				Remote		0.23–1.20	116–344	12–224	Dommergue et al. (2010)

ACPD
15, 11925–11983, 2015

Table 2. GEM/CO ratios in air plumes originated from mainland China.

Source region	GEM/CO ratio ($pg\,m^{-3}\,ppb^{-1}$)	Time	Receptor station	Reference
Eastern, Northern, and Northeast China	6.2 (n = 13)	Spring 2001	Flight over East Asia	Friedli et al. (2004); Pan et al. (2006)
Eastern China	6.5 (n = 2)	Summer 2004	Hedo station, Japan	Jaffe et al. (2005)
Eastern China	4.6 ± 1.3 (n = 10)	Apr 2004–Apr 2005	MBO, USA	Weiss-Penzias et al. (2007)
Eastern China	5.2 ± 4.3 (n = 68)	Feb 2005–Dec 2006	Seoul, Korea	Choi et al. (2009)
Southern China	5.0	Apr 2007	Mt. Lulin, Taiwan	Sheu et al. (2010)
Northern and Eastern China	11.4	Oct 2007	Mt. Lulin, Taiwan	
Eastern China	3.0	May 2006–May 2007	Jeju Island, Korea	Nguyen et al. (2010)
Northwest, Southwest, and Southern China	11.4	May 2005–Mar 2007	Flight over China	Slemr et al. (2009)
Northwest, Southwest, and Southern China	8.2 (n = 101)	May 2005–Jun 2013	Flight over China	Slemr et al. (2014b)
Northwest China	9.4 ± 3.5 (n = 20)	Oct 2007–Sep 2009	Mt. Waliguan, China	Fu et al. (2014b)
Southwest China	3.5 ± 2.6 (n = 3)	Jul–Oct 2010	Shangri-La, China	
Southwest China	6.1 ± 4.2 (n = 15)	Sep 2011–Mar 2013	Mt. Ailao, China	
Overall mean	6.7 ± 2.8			

ACPD
15, 11925–11983, 2015

Table 3. Hg concentrations and deposition fluxes of precipitation, throughfall, and litterfall in China and other regions worldwide. (Precipitation: * indicates bulk precipitation and the rest indicates wet-only precipitation. Mt. Gongga: [a] Elevation of the sampling site was 1600 m a.s.l., [b] Elevation of the sampling site was 3000 m a.s.l.)

Site	Location			Type	Study period		Hg Concentration ($ng\,L^{-1}$ $ng^{-1}\,g^{-1}$)		Deposition flux ($\mu g\,m^{-2}\,yr^{-1}$)		References
	Lon	Lat	Altitude (m a.s.l.)				THg	MeHg	THg	MeHg	
Mt. Ailao, Yunnan	101.02	24.53	2500	Remote	Jun 2011–May 2012	Precipitation	3.0		5.4		Zhou et al. (2013)
						Littefall	54.0		71.2		
Mt. Leigong, Guizhou	108.20	26.39	2178	Remote	May 2008–May 2009	Precipitation	4.0	0.04	6.1	0.06	Fu et al. (2010b)
						Throughfall	8.9	0.1	10.5	0.12	
						Littefall	91.0	0.48	39.5	0.28	
Mt. Damei, Zhejiang	121.57	29.63	550	Remote	Aug 2012–Jul 2013	Precipitation	4.1		7.0		(Lang, 2014)
						Littefall	46.6		26.0		
Nam Co, Tibet	90.99	30.77	4730	Remote	Jul 2009–Jul 2011	Precipitation	4.8	0.03	1.75	0.01	Huang et al. (2012)
Mt. Gongga[a], Sichuan	102.12	29.65	1640	Remote	Jan–Dec 2006	Precipitation*	9.9		9.1		Fu et al. (2008c)
Mt. Gongga[b], Sichuan	101.93	29.58	3000	Remote	May 2005–Apr 2005	Precipitation*	14.2	0.16	26.1	0.30	Fu et al. (2010a)
						Throughfall	40.2	0.3	57.1	0.43	
						Littefall	35.7		35.5		
Mt. Changbai, Jilin	128.47	42.40	750	Remote	Aug 2005–Jul 2006	Precipitation*	13.4		8.4		Wan et al. (2009a)
Puding, Guizhou	105.80	26.37	1145	Remote	Aug 2005–Jul 2006	Precipitation*	20.6	0.18	24.8	0.22	Guo et al. (2008)
Hongjiadu, Guizhou	105.85	26.88	1130	Remote	Aug 2005–Jul 2006	Precipitation*	39.4	0.18	34.7	0.16	
Yinzidu, Guizhou	106.12	26.57	1088	Remote	Aug 2005–Jul 2006	Precipitation*	35.7	0.18	38.1	0.19	
Dongfeng, Guizhou	106.13	26.85	970	Remote	Aug 2005–Jul 2006	Precipitation*	37.4	0.20	36.3	0.19	
Wujiangdu, Guizhou	106.77	27.32		Remote	Aug 2005–Jul 2006	Precipitation*	57.1	0.25	39.6	0.17	
Guiyang	106.72	26.57	1040	Urban	Jul–Sep 2008	Precipitation	13.3	0.05	13.4	0.05	Liu et al. (2011)
Xiamen	118.31	24.60	50	Urban	Jul 2013–Feb 2014	Precipitation	26.6				Wu (2014)
Chongqing				Urban	Jun 2010–Jun 2011	Precipitation	30.7	0.31	28.7	0.28	Wang et al. (2012, 2014c)
Tieshanping, Chongqing	104.683	29.633	500	Urban	Mar 2005–Mar 2006	Precipitation	32.3		29.0		Wang et al. (2009)
						Throughfall	69.7		71.3		
						Littefall	105		220		
Nanjing	118.78	32.05	100	Urban	Jun 2011–Feb 2012	Precipitation	52.9		56.5		Zhu et al. (2014)
North America				Urban		Precipitation	7.8–15.0		8.4–17.2		Mason et al. (2000); Keeler et al. (2005); Prestbo and Gay (2009)
				Remote		Precipitation	4.9–22.4	0.12	2.5–21.5	0.09	Rea et al. (2001); St Louis et al. (2001); Demers et al. (2007); Choi et al. (2008); Prestbo and Gay (2009); Fisher and Wolfe (2012)
						Throughfall	6.6–20.7	0.22	1.6–12.0	0.09	
						Litterfall	32.0–57.0	0.06–0.55	7.2–15.0	0.01–0.24	
Europe				Remote		Precipitation	11.9–18.0		7.0–36.0		Munthe et al. (1995); Lee et al. (2000); Schwesig and Matzner (2000); Wangberg et al. (2007); Larssen et al. (2008)
						Throughfall	22.8–29.0		15.0–39.0		
						Litterfall	28.0–68.0		4.0–32.5		

ACPD
15, 11925–11983, 2015

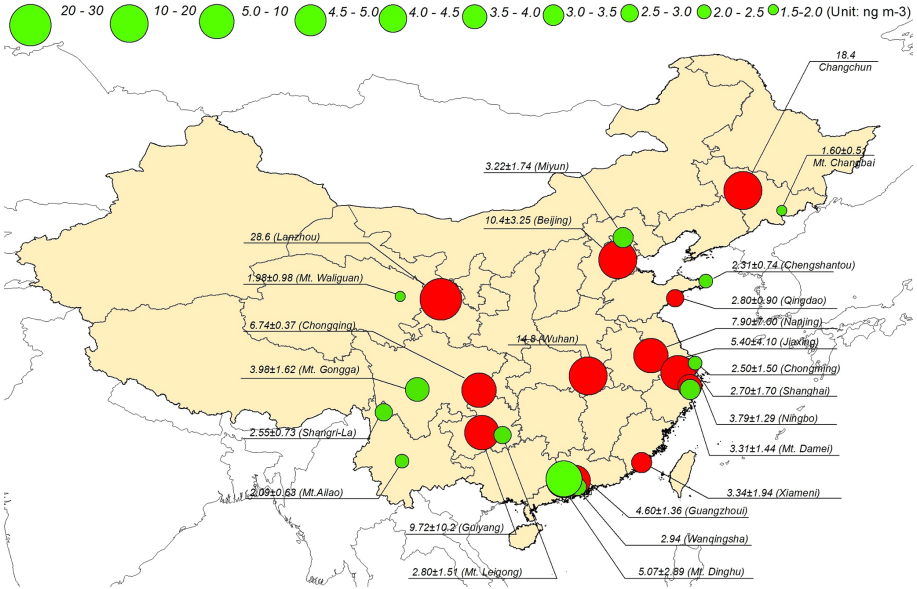

Figure 1. A map showing the locations and atmospheric GEM concentrations of the ground-based sites in mainland China (green and red circles indicate remote and urban sites, respectively, datasets were cited from literatures in Table 1).

ACPD
15, 11925–11983, 2015

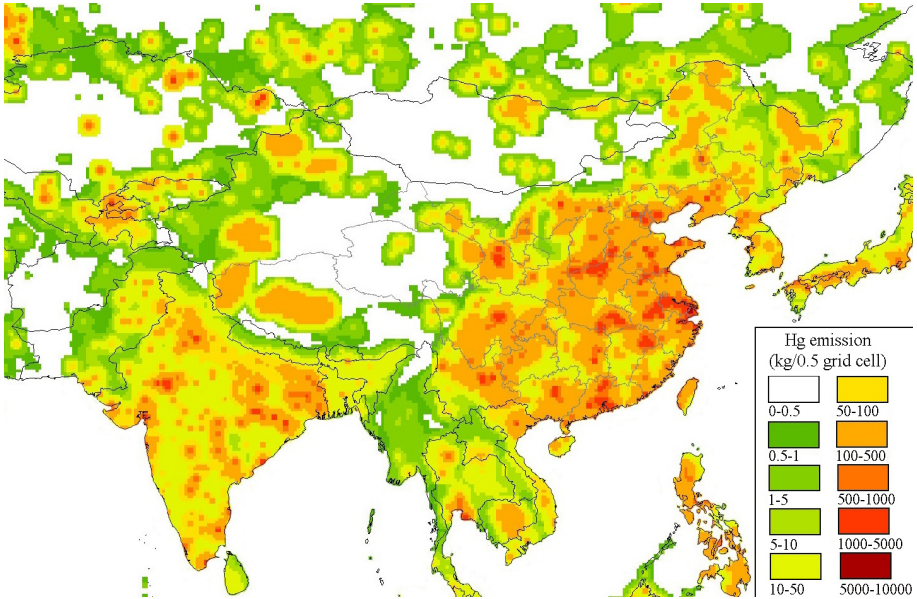

Figure 2. Anthropogenic total mercury emissions in East Asia (AMAP/UNEP, 2013).

ACPD
15, 11925–11983, 2015

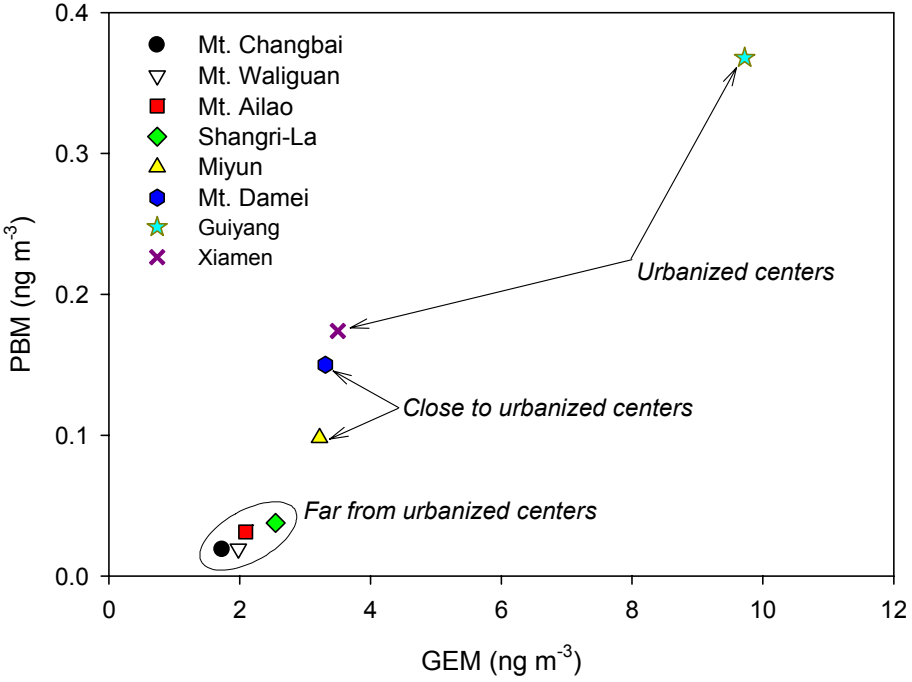

Figure 3. A correlation between atmospheric gaseous elemental mercury (GEM) and particulate bounded mercury (PBM, Hg-$P_{2.5}$) concentrations in remote and urban areas of China.

ACPD
15, 11925–11983, 2015

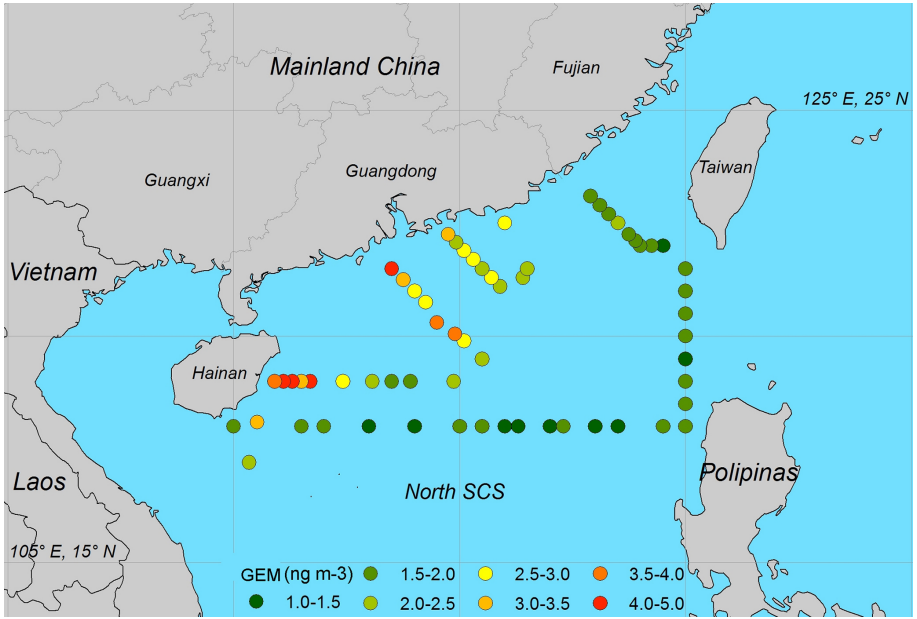

Figure 4. Spatial distribution of boundary layer GEM concentrations in the North South China Sea (Fu et al., 2010c).

ACPD
15, 11925–11983, 2015

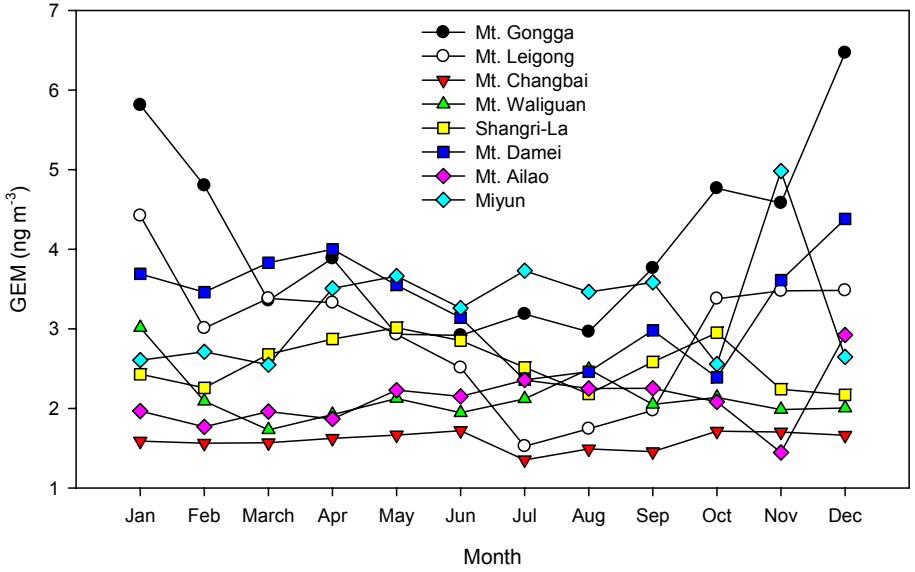

Figure 5. Monthly mean atmospheric gaseous elemental mercury (GEM) concentrations at remotes sites of China.

ACPD
15, 11925–11983, 2015

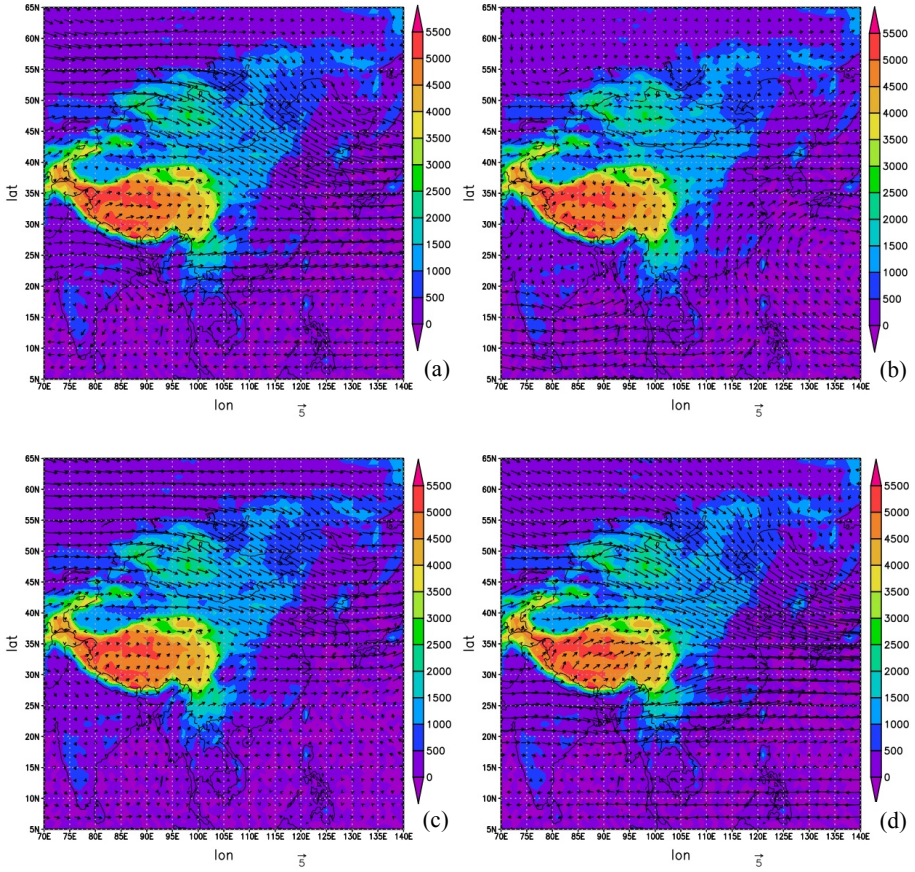

Figure 6. Wind field at 650 hPa level and Geopotential height during 2011–2013 in **(a)** spring, **(b)** summer, **(c)** autumn, and **(d)** winter. It was calculated using the Grid Analysis and Display System (GrADS) and gridded meteorological data (1.0° × 1.0°) from NCEP FNL (Final) Operational Global Analysis system.

ACPD
15, 11925–11983, 2015

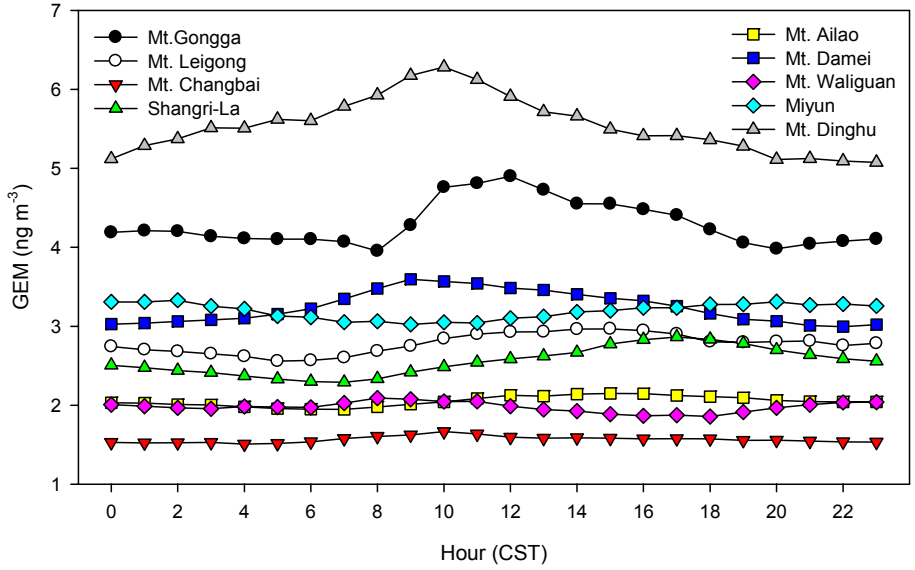

Figure 7. Diurnal trends of atmospheric gaseous elemental mercury (GEM) concentrations at remote sites of China.

ACPD
15, 11925–11983, 2015

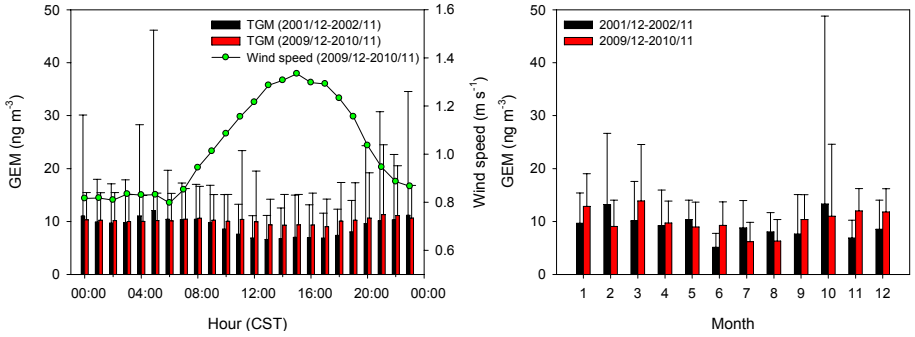

Figure 8. Comparisons of the diurnal and monthly trends of atmospheric gaseous elemental mercury (GEM) concentrations between the sampling years of 2001–2002 and 2009–2010 in Guiyang, southwest China (Fu and Feng, 2015).

ACPD
15, 11925–11983, 2015

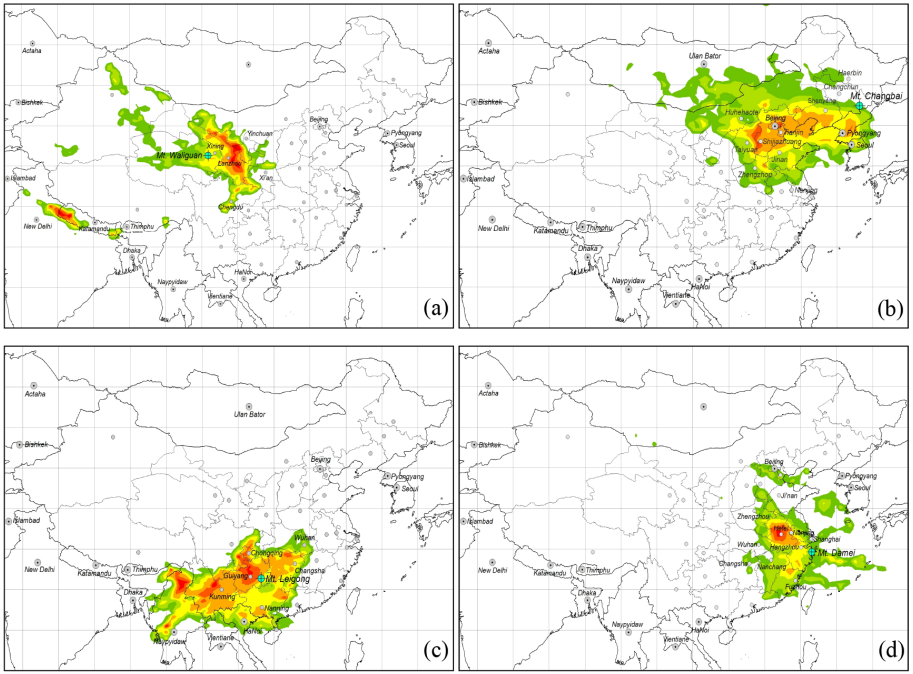

Figure 9. Potential source regions of atmospheric gaseous elemental mercury at **(a)** Mt. Waliguan, **(b)** Mt. Changbai, **(C)** Mt. Leigong, and **(d)** Mt. Damei (Fu et al., 2010b, 2012a, b; Yu et al., 2015).

ACPD
15, 11925–11983, 2015